UNIVERSITY OF NAPLES "FEDERICO II"

XXIV Cycle

PhD Program in Neuroscience

School of Molecular Medicine

A Hyperfunctional NCX3-Proteolytic Fragment Generated by $A\beta_{1-42}$ Delays Caspase-12 Activation and Neuronal Death in Mice

Coordinator:

Prof. Lucio Annunziato

Tutor:

Dr. Anna Pannaccione

PhD student:

Carla D'Avanzo

ACADEMIC YEAR 2010-2011

SUMMARY

1. INTRODUCTION

1.1 Alzheimer's disease

With an estimated 35 million afflicted world wide and a projected increase to 41 million in 2040 (Sloane *et al.* 2002), Alzheimer's disease (AD) is a late-onset progressive neurodegenerative disorder that leads to death within 3 to 9 years after diagnosis.

AD results in the irreversible loss of cholinergic cortical neurons, particularly in the associative neo-cortex and hippocampus. The principal risk factor for AD is age. With the increasing longevity of our population, AD is already approaching epidemic proportions with no cure or preventative therapy available (Hebert *et al.* 2000).

Clinically, AD is characterized by the progressive impairment of higher cognitive function, loss of memory and altered behaviour that follows a gradual progression. The pathological AD hallmarks are characterised at autopsy; the presence of senile plaques composed of extracellular amyloid-beta (Aβ) protein aggregates, intracellular neurofibrillary tangles (NFTs) composed of hyper-phosphorylated tau (τ) protein deposits, and the shrinkage of the cerebral cortex due to extensive neuronal loss. The "**amyloid cascade hypothesis"** remains the main pathogenetic model, as suggested by familial AD, mainly associated with mutation in amyloid precursor protein and presenilin genes (Querfurth and LaFerla 2000).

1.1.1 Protein Abnormalities in Alzheimer's Disease: Aβ and Tau Protein

The pathological AD hallmarks are the presence of cerebral senile plaques composed of extracellular amyloid-beta (Aβ) protein aggregates, intracellular neurofibrillary tangles (NFTs) composed of hyperphosphorylated tau (τ) protein deposits, and the shrinkage of the cerebral cortex due to extensive neuronal loss. The β-site amyloid precursor protein–cleaving enzyme 1 (BACE1 or β-secretase), the

principal actor in amyloid precursor protein (APP) processing in AD (Hayley *et al.* 2009), is a stress-response protein involved in several neurologic diseases including stroke (Wen *et al.* 2004), amyloid angiopathy, inflammation, and oxidative damage.

Aβ peptides are natural products of metabolism consisting of 36 to 43 amino acids. Monomers of $A\beta_{40}$ are much more prevalent than the aggregation-prone and damaging $A\beta_{42}$ species. Aβ peptides originate from proteolysis of the APP by the sequential enzymatic actions of BACE-1 and γ-secretase, a protein complex with presenilin-1 at its catalytic core (Haass and Selkoe 2007) (Fig. 1). An imbalance between production and clearance causes an aggregation and accumulation of Aβ peptides triggering AD. This process, called "**amyloid cascade hypothesis**", remains the main pathogenetic model, as suggested by familiar AD, mainly associated with mutation in APP and presenilin genes (Selkoe 2001; Tanzi *et al.* 2005) including Down's syndrome (Busciglio *et al.* 2002). Aβ peptides spontaneously self-aggregate into multiple coexisting forms. One form consists of oligomers (2 to 6 peptides), which link into intermediate assemblies (Kayed *et al.* 2003; Klein *et al.* 2001) (Fig. 1). Aβ peptides can also grow into fibrils, which arrange themselves into β-pleated sheets to form the insoluble fibers of advanced amyloid plaques. Soluble oligomers and intermediate amyloids are the most neurotoxic forms of Aβ (Walsh and Selkoe 2007). The severity of the cognitive defect in AD correlates with levels of oligomers in the brain, not the total Aβ (Lue *et al.* 1999).

Experimental evidence indicates that Aβ accumulation precedes and drives tau aggregation (Oddo *et al.* 2003; Gotz *et al.* 2001; Lewis *et al.* 2001). Tau is normally an abundant soluble protein in axons that promotes assembly and stability of microtubules and vesicle transport. Hyperphosphorylated tau is instead insoluble, lacks affinity for microtubules, and self-associates into paired helical filament structures. Like Aβ oligomers, the aggregates of abnormal tau molecules (neurofibrillary tangles) are cytotoxic and impair cognition. These filamentous inclusions are sited in pyramidal neurons and their number is a pathologic marker of the severity of AD.

Increased oxidative stress, the impaired protein-folding function of the endoplasmic reticulum (ER), and deficient proteasome-mediated and autophagic-mediated clearance of damaged proteins — all of which are also associated with

aging — accelerate the accumulation of amyloid and tau proteins in AD (López Salon *et al.*, 2000; Hoozemans *et al.* 2005).

1.1.2 APP processing and Aβ generation

Aβ peptides are produced by endoproteolysis of the parental APP, which is achieved by the sequential cleavage of APP by groups of enzymes or enzyme complexes named α-, β- and γ-secretases (Fig. 1). Three enzymes with α-secretase activity have been identified, all belonging to the ADAM family (a disintegrin- and metalloproteinase-family enzyme): ADAM9, ADAM10 and ADAM17 (Allinson *et al.* 2003). Several groups identified BACE1, which is a type I integral membrane protein belonging to the pepsin family of aspartyl proteases, as the β-secretase (Vassar *et al.* 1999; Hussain *et al.* 1999; Sinha *et al.* 1999). The γ-secretase has been identified as a complex of enzymes composed of presenilin 1 or 2, (PS1 and PS2), nicastrin, anterior pharynx defective and presenilin enhancer 2 (Wolfe *et al.* 1999; Steiner *et al.* 2002; Francis *et al.* 2002; Levitan *et al*. 2001; Yu *et al.* 2000).

The cleavage and processing of APP can be divided into a "**non-amyloidogenic pathway"** and an "**amyloidogenic pathway"**.

In the prevalent non-amyloidogenic pathway, APP is cleaved by the α-secretase at a position 83 amino acids from the carboxyl (C) terminus, producing a large amino (N)-terminal ectodomain (sAPPα) which is secreted into the extracellular medium (Kojro and Fahrenholz 2005). The resulting 83-amino-acid C-terminal fragment (C83) is retained in the membrane and subsequently cleaved by the γ-secretase, producing a short fragment termed p3 (Haass *et al.* 1993). Importantly, cleavage by the α-secretase occurs within the Aβ region, thereby precluding formation of Aβ.

The amyloidogenic pathway is an alternative cleavage pathway for APP which leads to Aβ generation. The initial proteolysis is mediated by the β-secretase at a position located 99 aminoacids from the C-terminus. This cut results in the release of sAPPβ into the extracellular space, and leaves the 99-amino-acid C-terminal fragment (known as C99) within the membrane, with the newly generated N-terminus corresponding to the first aminoacid of Aβ. Subsequent cleavage of this fragment (between residues 38 and 43) by the γ-secretase liberates an intact Aβ peptide. Most

of the full-length Aβ peptide produced is 40 residues in length ($A\beta_{40}$), whereas a small proportion (approximately 10%) is the 42 residue variant ($A\beta_{42}$). The $A\beta_{42}$ variant is more hydrophobic and more prone to fibril formation than $A\beta_{40}$ (Jarrett *et al.* 1993), and it is the longer form that is also the predominant isoform found in cerebral plaques (Younkin 1998).

Mutations in three genes — *APP*, *PS1* and *PS2* — are known to cause autosomal dominant AD, which generally manifests with an early-onset pathogenesis (St George-Hyslop, P. H. & Petit 2005). All these mutations affect the metabolism or stability of Aβ. These genetic mutations have been used to generate transgenic mouse models of the AD. One common mutation in APP is known as the Swedish mutation (APPSwe), in which a double amino acid change leads to increased cleavage of APP by the β-secretase (Haass *et al.* 1995). Other mutations, such as the Arctic mutation (APPArc), increase the aggregation of Aβ, leading to early onset, aggressive forms of the disease (Nilsberth *et al.*, 2001). Mutations in the presenilins, such as the PS1M146V mutation, increase levels of $A\beta_{42}$ (Guo *et al.* 1999; Jankowsky *et al.*, 2004), which aggregates more readily than $A\beta_{40}$. Increased dosage of the *APP* gene also results in AD (Gyure *et al.*, 2001; Mori *et al.* 2002).

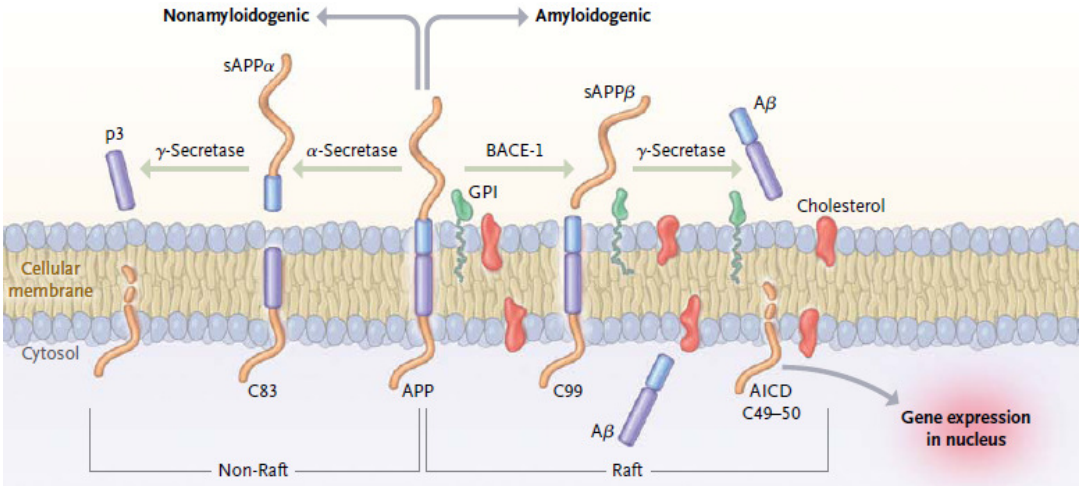

Fig. 1 APP processing: amyloidogenic pathway and non-amyloidogenic pathway

1.1.2.1 Intracellular Aβ

The Aβ peptide was first identified as a component of extracellular amyloid plaques in the mid-1980s. Not long thereafter, reports describing the existence of the intracellular Aβ began to appear in the literature. In the first study reporting the presence of intraneuronal Aβ, an antibody against residues 17–24 of Aβ was used, and Aβ-immunoreactive material was observed in neurons from the cerebellum, cerebrum and spinal cord of individuals with or without AD neuropathology (Grundke-Iqbal *et al.* 1989). As the participants in this study ranged in age from 38 to 83 years, these findings suggested that the occurrence of intracellular Aβ might not be an age-dependent event. Careful studies using C-terminal-specific antibodies against $A\beta_{40}$ and $A\beta_{42}$ have established that most of the intraneuronal Aβ ends at residue 42 and not at residue 40.

Despite the numerous publications in a range of animal species indicating that Aβ may accumulate intracellularly, the acceptance of this concept has been slow and controversial, mainly for technical reasons. One understandable objection relates to the extent of antibody cross-reactivity, as it is plausible that Aβ-specific antibodies may also recognize full-length APP or its other derivatives.

Recent studies suggest that the buildup of intracellular Aβ may be an early event in the AD pathogenesis. The accumulation of intraneuronal Aβ is an early event in the AD progression, preceding the formation of extracellular Aβ deposits. Indeed, it has been demonstrated that intraneuronal Aβ levels decrease as extracellular plaques accumulate (Mori *et al.* 2002). Curiously, authors reported that intraneuronal Aβ was not predictive of brain amyloidosis or NFT degeneration.

1.1.2.2 Intracellular sites of Aβ production

Although there is a large body of evidence to demonstrate that Aβ accumulates intracellularly, a key question that remains to be addressed is whether the intracellular Aβ builds up because a portion of the generated Aβ is not secreted and consequently remains intracellular, or alternatively, whether secreted Aβ is taken back up by the cell to form these intracellular pools (LaFerla *et al.* 2002). To address

these issues, it is important to understand how and where Aβ is cleaved and released from APP.

APP localizes to the plasma membrane (Kinoshita *et al.*, 2003) and is involved in cell adhesion (Breen *et al.*, 1991) and cell movement (Sabo *et al.*, 2001), but APP has also been localized to the trans-Golgi network (Xu *et al.*, 1991), ER, and endosomal, lysosomal and mitochondrial membranes (Mizuguchi *et al.*, 1992). The formation of Aβ could potentially occur in several cellular compartments where APP and the β- and γ-secretases are localized. The majority of Aβ is secreted, suggesting that Aβ is predominantly produced at the plasma membrane, or as part of the secretory pathway, so that it is rapidly expelled from the cell.

It has been shown that retention of APP in the ER blocks production of $A\beta_{40}$ but not $A\beta_{42}$, suggesting that $A\beta_{42}$ can be produced in the ER (Cook *et al.,* 1997; Lee *et al.*, 1998; Skovronsky *et al.*, 1998; Wild-Bode *et al.,* 1997).

Interestingly, these sites of Aβ production were limited to neurons, as in non-neuronal cells both $A\beta_{40}$ and $A\beta_{42}$ were produced at the cell surface rather than intracellularly (Hartmann *et al.*, 1997).

1.1.3 ER stress in AD

The ER is a membrane-enclosed reticular network connecting the nuclear envelope to the Golgi complex (Baumann *et al.* 2001). It has multiple vital functions: (I) protein folding, post-translational modification, and transport to the Golgi complex, (II) maintenance of cellular calcium homeostasis, (III) synthesis of lipids and sterols, and (IV) regulation of cellular survival via a complex transducer and signaling network (Baumann *et al.*, 2001; Gorlach *et al.*, 2006; Schroder *et al.*, 2005; Bernales *et al.*, 2006; Ron *et al.*, 2007; Kim *et al.*, 2008).

ER is a sensitive organelle which can recognize disturbances in cellular homeostasis and therefore it is not surprising that AD brains display many indications of ER stress (Hoozemans *et al.* 2009). ER can defend the host by activating the UPR (unfolded protein response) including signaling cascades that evoke the adaptive changes in metabolism and gene expression required to manage stress situations.

Should a condition become more prolonged or overwhelming, the ER can then trigger the apoptotic program killing the cell, but saving the tissue from necrotic injury.

Only caspase-4 and caspase-12 are activated by ER stress, their function in ER stress is still not defined (Martinon *et al.* 2009; Nadiri *et al.* 2006). Several studies have indicated that activation of caspase-12 is related to ER stress-induced apoptotic cell death. However, the activation mechanism is still unknown although some putative mechanisms have been proposed.

1.1.3.1 Neuronal ER stress: cause or consequence of AD?

Immunohistochemical studies have revealed that neurons in postmortem brain samples of AD patients display prominent expression of markers of ER stress. This is not a surprising result since AD involves several characteristics that could be inducers of ER stress, e.g. oxidative stress, accumulation of neurofibrillary tangles and even intraneuronal Aβ aggregates (Selkoe 2001; Tanzi *et al.* 2005; LaFerla *et al*. 2007). However, there is uncertainty about whether this neuronal ER stress triggers inflammation and AD pathology or whether it is a consequence of pathological processes in AD brain.

Genetic studies strongly indicate that Aβ production, oligomerization and aggregation have a crucial role in the pathogenesis of AD (Haass and Selkoe 2007; Selkoe 2001; Tanzi *et al.* 2005; LaFerla *et al.* 2007; Thinakaran *et al.* 2008). Recent studies have revealed that oligomers in particular are the toxic form of Aβ in AD pathogenesis. One key question is whether synthesized APP is cleaved in ER and in this way could trigger Aβ oligomerization and subsequently an unfolding response in ER. BACE1 and γ-secretase are present in ER but it seems that normally Aβ is not cleaved in ER due to (I) the incompatible pH optimum, (II) the presence of BACE1 stabilizers, and (III) the protective acetylation of BACE1 (Ko and Puglielli 2009).

In addition, ER stress has been shown to increase the expression of BACE1 and thus trigger APP processing in ER. It seems that ER stress can disturb APP processing in neurons, acts synergistically with other inducers to stimulate UPR in neurons, and subsequently provokes AD pathology in the context of prolonged stress.

On the other hand, AD is known to involve several pathological changes that can trigger ER stress and in that way aggravate AD pathogenesis.

ER stress can also prepare neurons to undergo apoptotic cell death. Interestingly, recent studies have indicated that ER stress can also trigger inflammatory responses to defend brain tissue against necrotic injuries. This response seems to be an alarm type of response involving chemokines and cytokines to activate glial cells. Excessive and/or prolonged ER stress can be detrimental to neurons since a delayed defense decreases the viability of neurons and can shift the UPR response to switch on an apoptotic program. However, the ER is highly specialized in neurons and the level of ER stress can vary among different sub-compartments, e.g. in dendrites and axonal synapses. Initial evidence indicates that ER stress can trigger synaptic loss and axonal degeneration. In conclusion, ER stress involves all the elements that can aggravate the AD pathogenesis.

1.1.4 Mitochondrial Dysfunction

Aβ is a potent mitochondrial poison, it affects in particular the synaptic pool (Mungarro-Menchaca *et al.* 2002). In AD, the exposure to Aβ inhibits key mitochondrial enzymes in the brain and in isolated mitochondria (Hauptmann *et al.* 2006; Reddy *et al.* 2008).

Cytochrome *c* oxidase is specifically attacked by Aβ (Caspersen *et al.* 2005). Consequently, electron transport, ATP production, oxygen consumption, and mitochondrial membrane potential all become impaired. The increase in mitochondrial superoxide radical formation and conversion into hydrogen peroxide cause oxidative stress, release of cytochrome *c*, and apoptosis. The accumulation of Aβ within structurally damaged mitochondria isolated from the brains of patients with AD (Hirai *et al.* 2001) and transgenic brains (Caspersen *et al.* 2005) is consistent with other evidence of intraneuronal Aβ in AD (Gouras *et al.* 2005).

The antihistamine dimebolin hydrochloride, a putative mitochondrial stimulant, has been reported to improve cognition and behavior in patients with mild to moderate AD (Doody *et al.* 2008).

1.1.5 Oxidative Stress

Dysfunctional mitochondria release oxidizing free radicals causing considerable oxidative stress (Good *et al.* 1996; Smith *et al.* 1996). Experimental models show that markers of oxidative damage precede pathological changes (Nunomura *et al*. 2001). Aβ, a potent generator of reactive oxygen species (ROS) (Hensley *et al.* 1994) and reactive nitrogen species (RNS), (Combs *et al.* 2001) is a prime initiator of this damage.

Mitochondrial hydrogen peroxide readily diffuses into the cytosol to participate in metal ion–catalyzed hydroxyl radical formation. Stimulated microglia are a major source of the highly diffusible nitric oxide radical. These ROS and RNS damage several molecular targets. Peroxidation of membrane lipids yields toxic aldehydes (Keller *et al.* 1997), which impair critical mitochondrial enzymes (Hirai *et al.* 2001; Humphries and Szweda 1998). Other essential proteins are directly oxidized, yielding carbonyl and nitrated derivatives (Smith *et al.* 1997). Subsequently, increases in membrane permeability to calcium, other ionic imbalances, and impaired glucose transport aggravate the energy imbalance (Mark *et al.* 1997).

1.1.6 Inflammation

Activated microglia and reactive astrocytes localize to fibrillar plaques, and their biochemical markers are elevated in the brains of AD patients (Wyss-Coray and Mucke 2002). Initially, the phagocytic microglia degrade Aβ. However, chronically activated microglia release chemokines and a cascade of damaging cytokines — notably, interleukin-1, interleukin-6, and tumor necrosis factor α (TNF-α) (Akiyama *et al.* 2000). In common with vascular cells, microglia express receptors for advanced glycation end products, which bind Aβ, thereby amplifying the generation of cytokines, glutamate, and nitric oxide (Yan *et al.* 1996; Li *et al*. 2003). In experimental studies, chemokines promote the migration of monocytes from the peripheral blood into plaque-bearing brain (Simard *et al.* 2006). Fibrillar Aβ and glial activation also stimulate the classic complement pathway (McGeer *et al.* 2001).

The contradictory roles of microglia — eliminating Aβ and releasing proinflammatory molecules — complicate treatment (Fiala *et al*. 2005). Nonsteroidal anti-inflammatory agents have been reported to lower the risk of AD and slow progression of the disease, but only in prospective observational studies (McGree *et al.* 2007; Vlad *et al*. 2008).

1.2 Calcium

Loss of calcium (Ca^{2+}) regulation is common to several neurodegenerative disorders. In AD, elevated concentrations of cytosolic calcium ($[Ca^{2+}]_i$) stimulate Aβ aggregation and amyloidogenesis (Isaacs *et al.* 2006; Pierrot *et al.* 2004). The presenilins modulate Ca^{2+} balance. Presenilin mutations might disrupt Ca^{2+} homeostasis in ER (Leissring *et al*. 2000; Nelson *et al.* 2007). However, the main effect of the mutations is to increase $Aβ_{42}$ levels, which in turn increases Ca^{2+} stores in the ER and the release of Ca^{2+} into the cytoplasm (LaFerla 2002). The relevance of these mechanisms to sporadic AD is unclear. A chronic state of excitatory amino acid (glutaminergic) receptor activation is thought to aggravate neuronal damage in late-stage AD (Rothman and Olney 1995). Glutamate increases $[Ca^{2+}]_i$, which in turn stimulates calcium-release channels in the ER. Aβ forms voltage-independent, cation channels in lipid membranes (Arispe *et al.* 1993), resulting in Ca^{2+} uptake and degeneration of neuritis (Lin *et al.* 2001). Indirectly, glutamate activates voltage-gated calcium channels. The L-type voltage-gated calcium-channel blocker, MEM 1003, is in a phase 3 trial, and memantine, an NMDA-receptor blocker, is approved by the Food and Drug Administration.

1.2.1 Calcium regulation of Aβ production and linkage to AD

By screening genes located in known AD linkage regions, Philippe Marambaud and colleagues (2008) discovered a novel calcium-conducting channel, with polymorphisms associated with increased risk for the development of Sporadic AD (SAD) (Dreses-Werringloer *et al.* 2008).

They called this novel calcium channel Calcium Homeostasis Modulator 1 (CALHM1). It is a three-transmembrane domain containing glycoprotein. Expression of CALHM1 was found in all brain regions and cells of neuronal lineage. CALHM1 localized predominantly to the ER but also exists at the plasma membrane where it mediates a novel Ca^{2+} influx to the cytosol, which is unaffected by specific blockers of store-operated Ca^{2+} influx or voltage-gated calcium channels but inhibited by nonspecific cation channel blockers such as cobalt (Fig. 2). CALHM1 appears to exist as multimeric complexes, forming a functional ion channel, and has structural similarities with the NMDA receptor within the ion selectivity region.

Critically, Ca^{2+} influx through CALHM1 decreases Aβ production and is accompanied by increases in sAPPα. The mechanism underlying this effect has not been elucidated but presumably involves a calcium-dependent effect on an α-secretase, which are enzymes that are known to cleave APP 83 amino acids from the carboxyl terminus and can thereby prevent Aβ formation. Conversely, increases in Aβ occur after siRNA knockdown of endogenous CALHM1 in cells when combined with calcium influx.

Curiously, this observation is contradictory to the vast majority of studies published on cytosolic Ca^{2+} entry and Aβ production, which indicate that increasing Ca^{2+} influx into the cytosol, either from the extracellular media or from ER stores, increases Aβ production (Green *et al*. 2007). An unexplored possibility could be that CALHM1 and the polymorphism P86L variant (that decrease Ca^{2+} permeability and also increases Aβ) exert their effects on Aβ processing via their location in the ER rather than the smaller pool found on the plasma membrane, given that the vast majority of CALHM1 was localized to the ER. It is unknown whether CALHM1 forms a functional cation-conducting pore within the ER, which could facilitate Ca^{2+} influx or efflux from the stores (Green et al. 2008).

As the channel appears to be constitutively open (as membrane depolarization was not required for Ca^{2+} influx), it may exist as a potential leak channel at the ER, which would increase $[Ca^{2+}]_i$ and would be diminished by the P86L variant.

This finding would then be in agreement with previous studies showing how ER Ca^{2+} regulation modulates Aβ production.

The source of elevated basal $[Ca^{2+}]_i$ in neurites in close proximity to Aβ plaques was unexplored by the authors. Basal Ca^{2+} levels are tightly regulated by a number of calcium pumps and binding proteins, which sequester free cytosolic Ca^{2+} so that it cannot affect local enzymes and signaling cascades.

Calcium enters into the cytosol from the extracellular space through ionotropic receptor-operated (ligand-gated) channels (ROCs), voltage-operated Ca^{2+} channels (VOCCs), and also through store-operated calcium-entry channels. ROCs permeable to Ca^{2+} include the N-methylo-D-aspartate receptors (NMDARs), some a-amino-3-hydroxy-5-methylisoxazole- 4-propionate acid receptors (AMPARs). Calcium can also enter into the cytosol from intracellular stores such as the ER via IP3 and ryanodine receptors, as well as the mitochondria. When $[Ca^{2+}]_i$ increases are large, mitochondria become rapidly-sequestering Ca^{2+} buffers, ensuring protection against excess of Ca^{2+}(Collins *et al.* 2001; Giacomelli *et al.* 2007). Indeed, slower Ca^{2+} clearance is mediated by Ca^{2+} pumps and exchangers located at plasma membrane level. Ca^{2+} ions are pumped out against a concentration gradient of four orders of magnitude by a plasma membrane Ca^{2+} ATPase (PMCA). Ca^{2+} is also removed from the cytoplasm by Na^{+}/Ca^{2+} exchanger (NCX) located in the cell membrane; NCX has low affinity but high capacity for Ca^{2+} compared with PMCA (Secondo *et al*. 2007) for this it is perfectly suited to extruding large amounts of this ion.

Conversely, $[Ca^{2+}]_i$ is reduced via the presence of calcium-binding proteins, such as calbindin, acting as buffers, and also through the extrusion of Ca^{2+} either into intracellular stores, such as the ER via the sarco-endoplasmic reticulum ATPase (SERCA), or out across the plasma membrane via plasmalemmal calcium pumps and exchangers (Fig. 2).

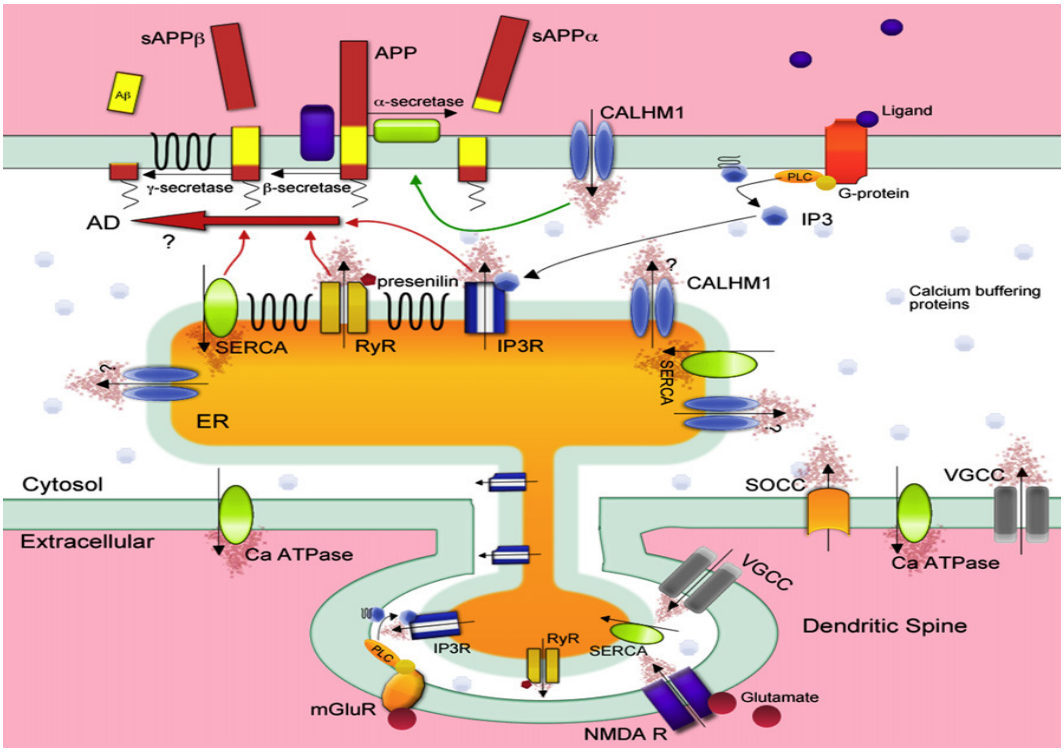

Fig. 2 Calcium Signaling Pathways

1.2.2 Presenilins and Calcium Homeostasis

Familial Alzheimer's Disease (FAD)-associated mutations in the presenilins were found to enhance IP_3-mediated Ca^{2+} release from the ER stores (LaFerla 2002). The presenilins were identified in 1995 as multi-transmembrane proteins, which predominantly localized to the ER, and were postulated to form a novel ion channel. Their involvement in the AD pathogenesis was cemented with the discovery that the presenilins formed the catalytic core of the γ-secretase complex, which liberates Aβ from the membrane fragment C99 (Fig. 1). These FAD mutations lead to the formation of the more predominantly 42 amino acid long version Aβ, which aggregates more readily.

The effects of FAD presenilin mutations on Ca^{2+} are very significant given that FAD presenilin mutations enhance Ca^{2+} release from the ER via the IP3 receptor (Leissring *et al*. 1999), the ryanodine receptor via caffeine (Smith *et al*. 2005), and through endogenous calcium leak channels (Tu *et al.* 2006), it was thought that these results could all be explained by an increase in ER Ca^{2+} load. However, the same

FAD-linked mutations have also shown a reduction in ER Ca^{2+} load and ER release with SERCA inhibition (Zatti *et al.* 2006). Thus, it is unclear whether all mutations increase ER Ca^{2+} or not.

Foskett and colleagues (2008) perfomed direct IP_3 channel recordings via single-channel patch-clamp electrophysiology of the ER membrane, expressing presenilin or FAD-linked mutants. Overexpression of mutant presenilin 1 or 2 directly increased IP3 channel activity by prolonging the channel open time (Cheung *et al* 2008).

Presenilin mutants appear to modulate the IP_3 receptors directly, as they were found to physically interact and are known to co-localize to the ER membrane (Ma *et al.* 2000).

Presenilin have been shown to interact with the ryanodine receptor, via its N terminus, and to increase the open channel probability and mean current (Rybalchenko *et al.* 2008), similar to that described with the IP3 receptor.

Furthermore to these ‘‘gain-of-function’’ interactions with native ER calcium receptors, FAD-linked presenilin mutations have also been shown to have a ‘‘loss-of-function’’ effect on ER Ca^{2+} dynamics by reducing endogenous Ca^{2+} leak from the ER (Tu *et al.* 2006).

Overexpression of wild-type presenilins also accelerates the sequestration of cytosolic Ca^{2+}, an effect that can be blocked by pharmacological inhibition of SERCA, suggesting that presenilins modulate SERCA function, and that SERCA pumping is impaired in the absence of both presenilins. Taken together, presenilins appear to interact and modulate Ca^{2+} influx into the ER via SERCA, and Ca^{2+} extrusion from the ER via interactions with the ryanodine and IP3 receptors.

ER Ca^{2+} regulation results to be a critical determinant for the production of Aβ, in addition to plasma membrane influx pathways such as with CALHM1.

1.3 The Sodium/Calcium Exchanger

The Na^+/Ca^{2+} exchanger (NCX) is one of the major means of Ca^{2+} extrusion at the plasma membrane of many excitable and non-excitable cells.

The regulation of Ca^{2+} and Na^+ homeostasis is a crucial physiological phenomenon in excitable cells. In fact, Ca^{2+} ions play a key role as a second

messenger in the cytosol and in the nucleus (Choi, 1988), while the Na^+ ion regulates the cellular osmolarity, induces action potentials (Lipton, 1999), and it is involved in the signal translation (Yu *et al.*, 1997). The control of this regulation is delegated to ionic channels selective for Ca^{2+} and Na^+, to Na^+ pumps, Ca^{2+} ATP-dependent and to NCX (Blaustein and Lederer 1999).

1.3.1 Molecular Biology of NCX

NCX belongs to the superfamily of membrane proteins comprising the following members:

1) the NCX family, which exchanges three Na^+ ions for one Ca^{2+} ion or four Na^+ ions for one Ca^{2+} ion depending on $[Na^+]_i$ and $[Ca^{2+}]_i$ (Reeves and Hale 1984; Fujioka *et al.* 2000; Hang and Hilgemann 2004);

2) the Na^+/Ca^{2+} exchanger K^+-dependent family, which exchanges four Na^+ ions for one Ca^{2+} plus one K^+ ion (Schnetkamp *et al.* 1989; Lytton *et al.* 2002);

3) the bacterial family which probably promotes Ca^{2+}/H^+ exchange (Cunningham KW and Fink 1996);

4) the nonbacterial Ca^{2+}/H^+ exchange family, which is also the Ca^{2+} exchanger of yeast vacuoles;

5) the Mg^{2+}/H^+ exchanger, an electrogenic exchanger of protons with Mg^{2+} and Zn^{2+} ions (Shaul *et al.* 1999).

These membrane proteins are all peculiarly characterized by the presence of α-repeats, the regions involved in ion translocation. Regarding the NCX family, three dominant genes coding for the three different NCX (Nicoll *et al.* 1990), NCX2 (Li *et al.* 1994), and NCX3 (Nicoll *et al.* 1996) proteins have been identified in mammals. These three genes appear to be dispersed, since NCX1, NCX2, and NCX3 have been mapped in mouse chromosomes 17, 7, and 12, respectively (Nicoll *et al.* 1996). At the post-transcriptional level, at least 12 NCX1 and 3 NCX3 proteins are generated through alternative splicing of the primary nuclear transcripts. These variants arise from a region of the large intracellular f-loop, are encoded by six small exons defined A to F, and are used in different combinations in a tissue-specific

manner. To maintain an open reading frame, all splice variants must include either exon A or B, which are mutually exclusive (Quednau *et al.* 1997).

NCX1 is composed of 938 amino acids in the canine heart and has a molecular mass of 120 kDa and contains nine transmembrane segments (TMS). NCX1 amino terminus (N-terminal) is located in the extracellular space, whereas the carboxyl terminus (C-terminal) is located intracellularly (Fig. 3). The nine transmembrane segments can be divided into an N-terminal hydrophobic domain, composed of the first five TMS (1–5), and into a C-terminal hydrophobic domain, composed of the last four TMS (6–9). These two hydrophobic domains are important for the binding and the transport of ions. The first (1–5) TMS are separated from the last four (6–9) TMS through a large hydrophilic intracellular loop of 550 amino acids, named the f-loop (Nicoll *et al* 1999). Although the f-loop is not implicated in Na^+ and Ca^{2+} translocation, it is responsible for the regulation of NCX activity elicited by several cytoplasmic messengers and transductional mechanisms, such as Ca^{2+} and Na^+ ions, NO, phosphatidylinositol 4,5 bisphosphate (PIP2), protein kinase C (PKC), protein kinase A (PKA), phosphoarginine (PA), and ATP. In the center of the f-loop, a region of approximately 130 amino acids in length (371–508 amino acids) has been reported to exert a Ca^{2+} regulatory function. This region is characterized by a pair of three aspartyl residues and by a group of four cysteines (Nicoll *et al.* 1999). At the N-terminal end of the f-loop near the membrane lipid interface, an autoinhibitory domain, rich in both basic and hydrophobic residues and consisting of a 20-aminoacid sequence (219–238), named exchange inhibitory peptide (XIP) (Matsuoka 1997), has been identified. The f-loop is also characterized by alternative splicing sites named α1-repeat and α2-repeat. The NCX protein amino acid sequence found between TMS2 and TMS3 is called α-1 repeat, whereas the one found between TMS7 and TMS8 is named α-2 repeat. With electrophoretic gels and under non reducing conditions, NCX1 migrates as a 120- and a 70-kDa band. The 120-kDa band represents the native protein, and the 70-kDa protein is a proteolytic fragment, which includes a large part of the f-loop and retains an NCX activity.

Interestingly, NCX2 and NCX3 have been found only in the brain and in the skeletal muscle. These two gene products consist of 921 and 927 amino acids and are characterized by molecular masses of 102 and 105 KDa, respectively. In

addition, NCX2 displays a 65% sequence identity with NCX1, whereas NCX3 possesses a 73% sequence identity with NCX1 and 75% sequence identity with NCX2 (Nicoll *et al.* 1996). All three NCX gene products share the same membrane topology.

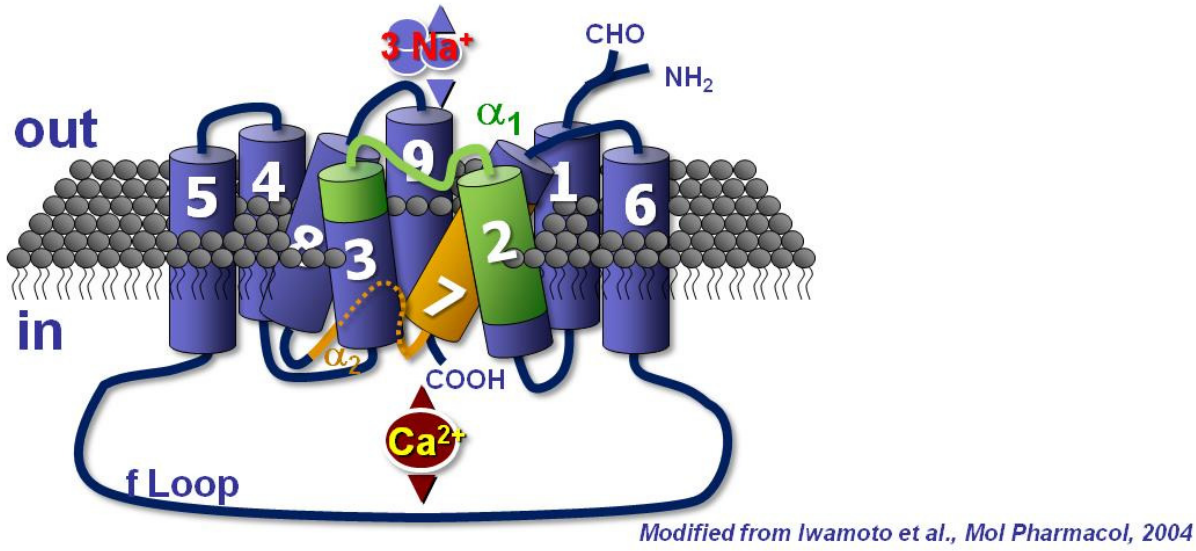

Fig.3 Molecular pharmacology of NCX.

NCX can facilitate both Ca^{2+} and Na^{+} flow in a bidirectional way through the plasma membrane (Blaustein and Lederer 1999; Philipson and Nicoll 2000) with a stoichiometry of 3 Na^{+} ions versus 1 Ca^{2+} ion.

Depending on the intracellular levels of Na^{+} and Ca^{2+}, NCX can operate in the forward mode by extruding one Ca^{2+} against three entering Na^{+}, using the Na^{+} gradient across the plasma membrane as a source of energy (Blaustein and Lederer 1999; Annunziato *et al.* 2004). Alternatively, in the reverse mode, NCX can function as Na^{+} efflux–Ca^{2+} influx. Because of its high exchange capacity, NCX is well-suited for rapid recovery from high intracellular Ca^{2+} concentrations ($[Ca^{2+}]_i$) and may play an important role in maintaining Ca^{2+} homeostasis and protecting cells from Ca^{2+} overload and eventual death (Blaustein and Lederer 1999; Annunziato *et al*. 2004).

1.3.2 NCX Regulation

Several factors are involved in the regulation of NCX activity: the two transported ions, Na^+ and Ca^{2+}, the intracellular pH, metabolic related compounds, ATP, PA, PIP2, PKA, and PKC, redox agents, hydroxyl radicals, H_2O_2, dithiothreitol (DTT), O^{2-}, Fe^{3+}, Fe^{2+}, Cu^{2+}, OH°, glutathione reduced (GSH), and glutathione oxidized (GSSG) and finally the gaseous mediator, NO.

1.3.2.1 Intracellular Ca^{2+} Concentrations

The site level at which $[Ca^{2+}]_i$ regulates NCX activity is different from the one required for Ca^{2+} transport. In fact, submicromolar concentrations (0.1– 0.3 μM) of intracellular Ca^{2+} are needed to activate the antiporter (Di Polo 1976; Hilgemann *et al* 1992). Indeed, the removal of intracellular Ca^{2+} ions completely blocks NCX activity (Philipson and Nicoll 2000). This regulatory function of low micromolar Ca^{2+} is more evident when the Na^+/Ca^{2+} exchanger is working in the reverse mode. However, it is not completely clear how low μM Ca^{2+} can also regulate NCX when it operates in the forward mode (Matsuoka *et al*, 1997). The location of such a regulatory site has been identified in the 134 amino acid length region, situated in the center of the intracellular f-loop. This region is characterized by a pair of three aspartyl residues and by a group of four cysteines.

1.3.2.2 Intracellular Na^+ Concentrations

In addition to the submicromolar intracellular Ca^{2+} regulatory site, an increase in $[Na^+]_i$ can also regulate the Na^+/Ca^{2+} exchanger (Hilgemann 1990). In particular, when intracellular Na^+ increases, it binds to the transport site of the exchanger molecule, and after an initial fast outward Na^+/Ca^{2+} current, an inactivation process occurs (Hilgemann *et al*. 1992). This inactivation process, very similar to the phenomenon occurring in voltage-dependent ionic channels, is named Na^+-dependent inactivation. The region of the intracellular f loop, in which this regulatory

site is located, has been identified in a 20-amino acid portion of the N-terminal part of the loop termed XIP (Matsuoka *et al.* 1997). Studies *in vitro* have characterized a negatively charged region of the intracellular f loop (445–455 amino acids) of the NCX protein that is able to cross link with synthetic XIP, suggesting that this amino acid sequence constitutes the binding site of XIP. On the other hand, since deletion mutagenesis of amino acids 562 to 685 results in an exchange activity that is no longer regulated by XIP, it is likely that XIP interacts with residues 445 to 455 and with another region of the f loop located between residues 562 and 685. Indeed, this region is believed to be a Na^+ regulatory site. Regarding the mechanism by which XIP inhibits NCX activity, it has been proposed that when the XIP-binding site is ligand occupied, a conformational change is induced in the C-terminal portion of the f loop, resulting in the inhibition of the ion transport. XIP is provided with relevant pharmacological implications. In fact, those exogenous peptides, having the same amino acid sequence as XIP, act as potent inhibitors of NCX activity (Pignataro *et al*. 2004). Interestingly, Ca^{2+} ions, at low micromolar concentrations, binding its regulatory site, decrease the extent of this Na^+-dependent inactivation. In fact, mutations in the Ca^{2+} regulatory binding site alter the activation and inactivation kinetics of exchange currents by modulating Na^+-dependent inactivation.

1.3.2.3 Intracellular H^+ Concentrations

H^+ strongly inhibits NCX activity under steady-state conditions. Changes in intracellular pH values, as little as 0.4, can induce a 90% inhibition of NCX activity. Since this H^+ ion modulatory action is α1-chymotrypsin sensitive, the action site of the proton can be attributed to the antiporter's hydrophilic intracellular loop (Annunziato *et al.* 2004). Intriguingly, such inhibitory action depends on the presence of intracellular Na^+ ions (Doering and Lederer 1994). Hence, the action exerted by H^+ ions is pathophysiologically relevant with regards to brain and heart ischemia. In fact, when intracellular H^+ and Na^+ ion homeostasis is deregulated, the anoxic conditions resulting in these cells may selectively interfere with the activity of the different NCX gene products. In particular, increases of H^+ and Na^+, as in anoxic conditions, sinergically inhibit NCX activity (Di Polo and Beauge 2002).

1.3.2.4 ATP, PKA, PKC, and PIP2

Acting as a phosphoryl donor molecule, ATP may increase the activity of the exchanger in a number of ways. Firstly, ATP directly participates in the NCX molecule phosphorylation process by PKA and PKC. Secondly, it increases PIP2 production. Finally, by activating G-protein-coupled receptors, via endogenous and exogenous ligands, ATP can stimulate the activity of the Na^+/Ca^{2+} exchanger through the pathway involving PKC or PKA activation (Annunziato *et al*. 2004). The mechanism underlying the phosphorylating effect on the exchanger seems to be related to an increase in its affinity for both internal Ca^{2+} and external Na^+ and to a decrease in its inhibition by internal Na^+. Each of the NCX isoforms has distinctive putative phosphorylation sites, although their roles have not yet been elucidated (Linck *et al.* 1998). ATP cellular depletion inhibits NCX1 and NCX2 but does not affect NCX3 activity. The exchange activity of NCX1 and NCX3 is modestly increased by those agents that activate PKA and PKC (Linck *et al.* 1998). More recently, the mechanism by which PKA and PKC activate NCX has been clarified. In fact, it has been demonstrated that the regulation of PKA-induced phosphorylation is due to the existence of an NCX1 macromolecular complex that contains the kinase PKA holoenzyme. This holoenzyme consists of two PKA catalytic subunits and two identical PKA regulatory subunits (Schulze *et al*. 2003). Together with PKA, other critical regulatory enzymes are also associated with NCX1, including PKC and serine-threonine protein phosphatases, PP1 and PP2A (Schulze *et al*. 2003). Particularly a pathway involving PKC has been shown to stimulate NCX1 (Iwamoto *et al.* 1996; Iwamoto *et al.* 1995). In a more recent paper, it has been demonstrated that PKC-dependent regulation of NCX isoforms also involves NCX3 but not NCX2 (Iwamoto *et al.* 1998). In the same paper, three phosphorylation sites in the NCX1 protein, Ser-249, Ser- 250, and Ser-357, have been identified. Among these, Ser-250 is the amino acid that is predominantly phosphorylated (Iwamoto *et al*. 1998). The other mechanism by which ATP can activate NCX occurs through PIP2 production. This mechanism of activation is related to the relevant PIP2 influence on Na^+-dependent inactivation of NCX. In fact, PIP2 directly interacts with the XIP region of

the exchanger, thus eliminating its inactivation and stimulating NCX function. Indeed, exchangers with mutated XIP regions no longer respond to PIP2 or to PIP2 antibodies (Hingelmann *et al*. 1992).

1.3.2.5 Redox Agents

In the last 15 years, several groups of investigators using different cellular models, such as cell-expressing cloned splicing variants of the brain, heart isoforms, cardiac sarcolemma vesicles, cells transiently transfected with NCX1 isoform, and giant excised patches, have found that the Na^+/Ca^{2+} exchanger is sensitive to different combinations of redox agents (Reeves *et al*. 1986; Amoroso *et al.* 2000). In particular, the stimulation of the exchange activity requires the combination of a reducing agent (DTT, GSH, or Fe^{2+}) with an oxidizing agent (H_2O_2 and GSSG). The effects of both agents are mediated by metal ions (e.g., Fe^{2+}). The antiporter's sensitivity to changes in the redox status can assume particular relevance during oxidative stress. In fact, in this condition, the modulation of reactive oxygen species (ROS) could affect the transport of Na^+ and Ca^{2+} ions through the plasma membrane.

1.3.2.6 Nitric Oxide

The ubiquitous gaseous mediator Nitric Oxide (NO) seems to be involved in the modulation of NCX activity. In fact, Asano *et al.* (1995) provided evidence that NO, released by NO donors, is able to stimulate NCX in the reverse mode of operation in neuronal preparations and astrocytes through a cGMP-dependent mechanism. In contrast, in C6 glioma cells, the stimulatory action on NCX reverse mode of operation, elicited by the NO donor sodium nitroprusside (SNP), is not elicited by NO release but by the presence of iron in SNP molecule (Amoroso et al. 2000). In addition, a direct relationship between the constitutive form of nitric oxide synthase (NOS), the enzyme involved in NO synthesis, and NCX has recently been demonstrated. Indeed, heat stress by inducing NOS phosphorylation causes NOS complexation with NCX, thus decreasing its activity. Very recently, we have

demonstrated the selectivity of NO in modulating each isoform at different molecular determinant level (Secondo *et al*. 2010).

1.3.3 NCX Role in Physiological Conditions

The NCX protein may play a relevant function in different neurophysiological conditions. In neurons, the level of expression of NCX is particularly high in those sites where a large movement of Ca^{2+} ions occurs across the plasma membrane, as it happens at the level of synapses (Annunziato *et al.* 2004). Specifically, during an action potential or after glutamate-activated channel activity, Ca^{2+} massively enters the plasma membrane. Such phenomenon triggers the fusion of synaptic vesicles with the plasma membrane and promotes neurotransmitter exocytosis. After this event, outward K^+ currents repolarize the plasma membrane, thus leading to VOCC closure. According to the diffusion principle, Ca^{2+} ions are distributed in the cytosolic compartment, reversibly interacting with Ca^{2+}-binding proteins. Residual Ca^{2+} is then rapidly extruded by the plasma membrane Ca^{2+} ATPase and by NCX.

The NCX becomes the dominant Ca^{2+} extrusion mechanism when $[Ca^{2+}]_i$ is higher than 500 nM, as it happens when a train of action potentials reaches the nerve terminals. It has been calculated that for these $[Ca^{2+}]_i$ values (500 nM), more than 60% of Ca^{2+} extrusion is mediated by NCX families. In such physiological conditions, NCX activation is consistent with its low-affinity (K_d=500 nM) and high-capacity (5 X 10^3 Ca^{2+}/s) function. In contrast, in resting conditions or after a single action potential, when $[Ca^{2+}]_i$ slightly increases, requiring, therefore, a more subtle control, the high-affinity (K_d=100 nM) and low-capacity (10^2 Ca^{2+}/s) pump, plasma membrane Ca^{2+}-ATPase, assumes a predominant function, thus making the involvement of NCX less relevant (Blaustein and Lederer 1999).

1.3.3.1 NCX genes knocking-out effect

ncx1-, *ncx2*- and *ncx3*-specific knockout mice were generated over the past decade (Jeon *et al*. 2003; Sokolow *et al*. 2004; Wakimoto *et al*. 2003).

These mouse models are useful tools for elucidating NCX1–3 specific function in physiological and pathophysiological processes in the central nervous system (CNS). NCX1-deficient mice are not viable. NCX1 null-mutation caused embryonic lethality, irregular heartbeats and apoptosis in the heart (Wakimoto *et al*. 2003; Koushik *et al*. 2001). Recent studies indicated that cardiac-specific transgenic re-expression of NCX1 was not enough to rescue the lethal phenotype, suggesting an important non-cardiac role for NCX1 during embryogenesis (e.g. vascularization of yolk sac, placental development) (Cho *et al*. 2003; Conway *et al.* 2002). Mice lacking NCX2 exhibit enhanced learning and memory (Jeon *et al*. 2003). Targeted disruption of NCX3 leads to defective neuromuscular transmission (Sokolow *et al*. 2004). Under ischemic conditions, NCX3-deficient mice exhibit increased neuronal damage (Molinaro *et al*. 2008; Cross *et al*. 2009). Studies also showed that NCX plays a major role in restoring baseline Ca^{2+} levels following glutamate-induced depolarization in cortical and hippocampal neurons (Jeon *et al*. 2003; Ranciat-McComb *et al.* 2000). These findings highlight NCX function in the regulation of Na^{+} and Ca^{2+} following synaptic activity.

1.3.4 NCX Role in Pathophysiological Conditions

The disregulation of $[Ca^{2+}]_i$ and $[Na^{+}]_i$ homeostasis is involved in neuronal and glial injury occurring in *in vitro* and *in vivo* models of hypoxia-anoxia and in several neurodegenerative diseases.

In a cellular model of glial cells, C6 glioma, the activation of NCX, in reverse mode, obtained by $[Na^{+}]_e$ removal, reduces cell injury induced by chemical hypoxia. Such phenomenon suggests that the antiporter plays a protective role during this pathophysiological condition. Consistent with these results, the pharmacological inhibition of NCX activity worsens cell damage by increasing the intracellular concentration of Na^{+} ions (Amoroso *et al*. 1997). Furthermore, the stimulation of NCX activity by redox agents results in a protective effect (Amoroso *et al*. 2000; Sirabella *et al*. 2009) against hypoxia as well as the overexpression of NCX3 (Secondo *et al.* 2007). Published evidence demonstrated that Ca^{2+} influx due to NCX activity in reverse mode is the main component of the excitotoxicity damage (Kiedrowski 1999).

More papers highlighted the different roles played by the different NCX isoforms in the cell survival modulation in cellular death models. For example, NCX3 is neuroprotective during an ischemia insult *in vitro* both in neuronal models and in cells transfected with only this isoform. This role is attributable to the NCX3 ability to buffer the cytosolic Ca^{2+} by the forward mode of operation, like during glutamate increase or chemical ipoxia insult (Secondo *et al*. 2007). In particular Bano *et al.* (2005) showed that NCX is cleaved by calpains in brain ischemia and in cultured cerebellar granule neurons exposed to glutamate. Calpains (Mellgren *et al*. 1989; Murachi *et al*. 1987) modulate a variety of physiological processes (Robles *et al*. 2003) but can also become important mediators of cell death (Neumar *et al.* 2003). Ample evidence documents the activation of calpains in brain ischemia and excitotoxic neuronal degeneration (Lankiewicz *et al.* 2000; Leist *et al*. 1997; Siman and Noszek 1988).

In *in vivo* models, reproducing human cerebral ischemia through the occlusion of the middle cerebral artery, the inhibition of NCX, induced by selective inhibitors (Pignataro *et al.* 2004) or by the knockout of one of the NCX isoforms (NCX2) (Jeon *et al*. 2003) or NCX3 (Molinaro *et al.* 2008) aggravates brain infarct, whereas the activation of the antiporter with redox agents reduces the cerebral infarctual area (Pignataro *et al.* 2004).

The role played by NCX in those neurons and glial cells involved in cerebral ischemia should be differentiated according to the anatomical regions involved in the ischemic pathological process. In particular, it is conceivable that, since in the penumbral region ATPase activity is still preserved, NCX may likely operate in a forward mode. As a result, by extruding Ca^{2+} ions, the exchanger favors the entry of Na^{+} ions. Therefore, the inhibition of NCX in this area reduces the extrusion of Ca^{2+} ions, thus enhancing Ca^{2+}-mediated cell injury. In contrast, in the ischemic core region, in which ATP levels are remarkably low and Na^{+}/K^{+} ATPase activity is reduced, intracellular Na^{+} ions massively accumulate because of Na^{+}/K^{+} ATPase failure (Boscia *et al*. 2006).

Hence, the intracellular Na^{+} loading promotes NCX to operate in the reverse mode as an Na^{+} efflux-Ca^{2+} influx pathway.

In conclusion, the NCX pharmacological inhibition in this core region further worsens the necrotic lesion of the surviving glial and neuronal cells as the loading of intracellular Na^+ increases (Pignataro *et al.* 2004).

The **"Ca^{2+} hypothesis"** provides an attractive mechanism to explain the cell death associated with AD. The theory proposes that cell death results from elevated $[Ca^{2+}]_i$.

The acute or chronic in $[Ca^{2+}]_i$ rise may exist lead the cell to an irreversible pathway of necrosis and/or apoptosis. If true, derangements in several Ca^{2+} homeostatic processes could simultaneously contribute to and be responsible for a persistent rise in $[Ca^{2+}]_i$. Peterson (1992) documents the many changes that occur in Ca^{2+} homeostatic processes in the aging brain and AD. A large bulk of studies have shown that the neurotoxicity exerted by Aβ protein is intimately related to $[Ca^{2+}]_i$. Indeed, the attenuation of $[Ca^{2+}]_i$ increase by Ca^{2+} channel blockers, growth factors, and cytochalasins results in a reduction of neural damage induced by the Aβ peptide. It has been demonstrated that exposure to the Aβ protein partially reduces Na^+-dependent Ca^{2+} accumulation in plasma membrane vesicles deriving from the human frontal cortex of patients affected by AD. These findings have suggested that Aβ directly interacts with the hydrophobic surface of the NCX molecule, thus interfering with plasma membrane Ca^{2+} transport (Yu *et al*. 1997).

Many evidence are in literature in support of the "Ca^{2+} hypothesis of AD". Where does the NCX become involved in this mechanism? NCX would be expected to be neuroprotective in situations where elevations in $[Ca^{2+}]_i$ are leading to cell death. This neuroprotective role was proposed to explain increased NCX activity in AD brain (Colvin *et al.* 1991). In this model, neurons that survived the neurodegenerative elevations in $[Ca^{2+}]_i$ caused by AD did so because they had increased capacity for NCX. This increased capacity for NCX in surviving neurons was manifested as increased Na^+-dependent Ca^{2+} uptake in plasma membrane vesicles derived from AD brain (Colvin *et al.* 1994).

Changes in the Ca^{2+} transport rate of the NCX in neurons could be caused by both changes in the NCX isoforms expression or in the lipid composition (Moson *et al.* 1992) of the plasma membrane.

The generation of NCX1–3 specific antibodies has allowed the study of their specific expression in terminals isolated from AD and cognitively normal individuals. Sokolow *et al*. (2011) demonstrated for the first time that selective changes occur in the pattern of NCX1–3 protein expression in AD synaptosomes. Major findings can be summarized as follows: (i) NCX1–3 are widely expressed in human synaptosomes isolated from parietal cortex of AD and control patients; (ii) NCX2 expression was modestly but significantly increased and NCX3 levels were significantly reduced in AD terminals compared to controls and (iii) all NCX isotypes co-localized with Aβ in AD parietal cortex. NCX1 is 1.5 times more abundant than NCX2 and NCX3 in the parietal cortex of cognitively normal patients. Quantitative flow cytometry also showed that NCX2 levels were increased and NCX3 levels reduced in the parietal cortex of AD patients. NCX2 up-regulation in AD terminals may be the result of a compensatory mechanism to balance the loss of NCX3 expression. A net increase of NCX proteins may result in increased NCX activity in AD brains (Colvin *et al*. 1994). The present experiments demonstrated co-localization of NCX1, NCX2 and NCX3 with Aβ, and all three NCX isoforms were up-regulated in pathological terminals that contained Aβ. Increased levels of NCX1, NCX2 and NCX3 in Aβ-positive terminals are likely to follow oligomeric Aβ–induced Ca^{2+} imbalance and may be an indication of the participation of NCX1–3 in Ca^{2+} homeostasis in surviving synapses affected by the intra-terminal toxicity of Aβ oligomers (Green *et al*. 2008).

The possibility that NCX is a substrate for caspases was suggested by the demonstration that in Western blot analysis the full-length 120-kDa NCX1 protein co-purifies with an active proteolytic fragment of 70 kDa (Philipson *et al*. 1988); this latter segment is likely to derive from a proteolytic cleavage at the level of two close sites of the NCX intracellular f-loop. More recently, Nicotera, Carafoli, and colleagues claimed that NCX1 can be cleaved by caspase 3 in cerebellar granule cells undergoing apoptosis, thus suggesting that NCX possesses consensus sites for caspases. As a result, the NCX cleavage operated by caspases might participate in the events leading neurons to switch from apoptosis to necrosis (Schwab *et al.* 2002). In fact, when cellular Ca^{2+} efflux is hindered by NCX failure, a Ca^{2+} overload occurs, shifting the balance of neuronal death from apoptosis to necrosis (Schwab *et al*. 2002).

Release of Ca^{2+} ions from internal calcium stores may gain access Ca^{2+} to the neuronal cytoplasm via ion channels or calcium transport systems, or through the release of Ca^{2+} ions from intracellular stores. Depletion of Ca^{2+} ions from the ER has been suggested as an initial signal for ER dysfunction in ischemic neurons. Many studies indicate that a strong release of calcium ions from ER is associated with damage to cells, including damage to neurons after ischemia. Deregulation of ER Ca^{2+} homeostasis following ischemia involves two phases: accumulation of Ca^{2+} in ER stores and subsequent release of Ca^{2+} from ER following ischemia/reoxygenation.

Consistent with an elevation of NCX activity and in accordance with normal [Ca^{2+}], Sirabella *et al*. (2009) showed that in primary cortical neurons, transcript and protein expression of the three isoforms, NCX1, NCX2, and NCX3, respond differently to anoxic injury. In particular, 3 hours of OGD (Oxygen Glucose Deprivation) induced an NF-kB-dependent up-regulation of NCX1 and a proteasomal-dependent NCX3 down-regulation, leaving, however, NCX2 unaffected. These changes in NCX isoform expression during OGD were accompanied by increases in NCX currents (I_{NCX}), both in the reverse and forward modes of operation, and by cytosolic Ca^{2+} levels comparable to those found under normoxic conditions. Consistent, with an elevation of NCX activity and in accordance with normal cytosolic [Ca^{2+}], they found that during OGD, an increased refilling of Ca^{2+} into ER occurred. This augmented refilling was prevented by NCX inhibition and by NCX1 knocking-down, thus suggesting that this plasma membrane antiporter is crucial for the Ca^{2+} refilling process. Interestingly, when this refilling process was prevented by the plasma membrane NCX blockade or by NCX1 knocking-down, an activation of caspase-12, a specific marker of ER stress, occurred together with an increased neuronal vulnerability to OGD. Altogether these data suggested the protective role played by NCX when it works in the reverse mode. In fact, the increase in free Ca^{2+} concentration, indeed by NCX, within the ER appears to be a protective key factor in that it determines the synthesis and processing of proteins within this organelle, a crucial early self-protective mechanism against ER stress. By contrast, its depletion activates neuronal cell death signals. Intriguingly, it is also well known that Ca^{2+} accumulation and NF-kB translocation into the nucleus constitute relevant self-

protective mechanisms against ER stress. Remarkably, whereas the transcriptional factor NF-kB, induced by ROS, was responsible for NCX1 up-regulation in cortical neurons exposed to OGD, the inhibition of its translocation into the nucleus prevented NCX1 overexpression. Unlike NCX1, the other brain-specific isoform NCX3 displayed a down-regulation during OGD that was not exerted at the transcriptional level but was rather proteasomal-dependent. Particularly, evidence that proteasome inhibition did not affect basal NCX3 expression suggests that this system is specifically activated by OGD. Interestingly, the proteasomal system appears to be involved in the early phase of ER stress as an upstream signal able to induce caspase and calpain activation. In addition to the effect of the proteasomal system, the NCX3 downregulation could also be ascribed to the activation of calpains involved in glutamate-induced excitotoxicity in cerebellar granule cells. However, current findings demonstrated that the inhibition of the proteasomal system completely prevented OGD-induced NCX3 down-regulation, thereby suggesting that under OGD, this degradation pathway is the only operative system.

In agreement with the data showing that there was an up-regulation of NCX1 expression, we found that the total I_{NCX} recorded in the reverse and forward modes of operation were higher than those in controls at 1 and 3 hours after OGD. However, the re-exposure of cortical neurons to 24 hours of reoxygenation significantly reduced I_{NCX} in the reverse mode. Noticeably, the enhancement of I_{NCX} began just 1 hour after OGD, a time when no increases in NCX1 protein expression were detected. This evidence suggested that this I_{NCX} increase was most likely due to an OGD-induced functional modulation rather than protein overexpression. This assumption was further confirmed by cytosolic Ca^{2+} variations observed during OGD. The increase in $[Ca^{2+}]_i$ after 1 hour of hypoxia was probably due to the increased activity of NCX in the reverse mode during the same time period, whereas its return to control levels after 3 hours of OGD was probably the result of NCX-dependent Ca^{2+} refilling into ER. In fact, this refilling was blocked by CB-DMB and by siRNA against NCX1. In agreement with these results, in anoxic astrocytes and in Ca^{2+} oscillating muscle cells, NCX blockade prevents ER Ca^{2+} refilling (Sirabella *et al.* 2009).

2. AIM OF THE STUDY

Owing to this evidence, by means of patch-clamp, Fura-2AM microfluorimetry, western blot, site-directed mutagenesis, deletions, and chimera strategies, we characterized:

(**a**) The $A\beta_{1-42}$-effects on the expression and the activity of NCX;

(**b**) The molecular mechanisms underlying $A\beta_{1-42}$-mediated effects on NCX isoforms;

(**c**) The molecular determinants responsible for $A\beta_{1-42}$-effects on NCX;

(**d**) The role of NCX isoforms in Ca^{2+}-refilling into ER, caspase-12 activation, apoptosis, and neuronal death induced by $A\beta_{1-42}$.

3. MATERIALS AND METHODS

$A\beta_{1-42}$ and mouse monoclonal anti-β-Actin (1:1000), as well as all other unmentioned materials, were from Sigma Chemicals (St. Louis, MO, USA). Nerve Growth Factor (NGF 2.5S) and Tetrodotoxin (TTX) were from Alomone Labs (Jerusalem, Israel). Rabbit polyclonal anti-Caspase12 (1:500) and goat polyclonal anti-Calpain (1:500) antibodies were purchased from Santa Cruz Biotechnology (Santa Cruz, California, USA). Rabbit polyclonal antibody anti-NCX3 (1:5000) was kindly provided by Dr K. D. Philipson and Dr D. A. Nicoll (Los Angeles, California, USA) whereas mouse monoclonal anti-NCX1 (1:1000) was from Swant (Bellinzona, Switzerland).

RPMI 1640, horse serum (HS), fetal bovine serum (FBS), Dulbecco's Modified Eagle's (DMED), Nutrient Mixture F-12 (Ham's F-12), L-glutamine, fetal calf serum (FCS), Earle's balanced salt solution (EBSS), and phosphate buffed saline (PBS) were from Gibco-BRL (Grand Island, NY, USA). Protease inhibitor cocktail II was purchased from Calbiochem (San Diego, CA, USA).

3.1 Cell cultures

3.1.1 BHK cells

The baby hamster kidney (BHK) cells, stably transfected with canine cardiac NCX1 or rat brain NCX3, were grown on plastic dishes in a mix of DMEM and Ham's F12 media (1:1) (Gibco, Invitrogen, MI, Italy) supplemented with 5% fetal bovine serum, 100U/ml penicillin, and 100µg/ml streptomycin. Cells were cultured in a humidified 5% CO_2 atmosphere; the culture medium was changed every 2 days. For microfluorimetric and electrophysiological studies, cells were plated on glass coverslips (Fisher, Springfield, NJ, USA) coated with poly-L-lysine (30µg/ml) and used at least 12 hours after plating (Secondo *et al*. 2007).

3.1.2 PC-12 cells

Rat pheochromocytoma cells (PC-12 cells) were grown as previously described (Pannaccione *et al*. 2005). For all the experiments, cells were seeded at low density on glass cover-slips coated with poly-L-lysine (50μg/ml). Differentiation of PC-12 cells was achieved by NGF 2.5S treatment (50ng/ml) for 7-9 days (Greene and Tischler 1976).

3.1.3 Mouse hippocampal neurons

Hippocampal neurons were obtained from the brains of 18-day-old C57BL/6 wild-type, *ncx3+/+*, and *ncx3–/–* mice embryos as previously described (Scorziello *et al*. 2001). Cytosine-β-D-arabino-furanoside (5μM) was added after 5 days of plating to prevent the growth of non-neuronal cells. In all experiments, neurons were cultured in a humidified atmosphere at 37°C with 5% CO_2, and used after 8 days of culturing (8DIV).

3.2 **Aβ_{1-42} peptide treatment**

Aβ_{1-42} was prepared as 0.1mg/0.1ml stock solution in sterile PBS incubated at 37°C for 24 hours to enhance aggregation**,** and stored at -20°C. Stock solution was then directly diluted in cell culture media to give the desired experimental concentrations (5μM).

3.3 **RNA Silencing**

The pSUPER.retro.puro vector (OligoEngine) was used to express siRNA against NCX1 (siNCX1) or NCX3 (siNCX3) in PC-12 cells. In particular, two complementary oligonucleotides were annealed and inserted into pSUPER.retro.puro according to the manufacturer's instructions. The gene-specific siNCX1 and siNCX3 contain the 19-nucleotide sequence corresponding to the nucleotides 2000-2018 and 124-142

downstream of the transcription start site of rat NCX1 (GenBank accession no. NM_019268) and of rat NCX3 (GenBank accession no. U53420), respectively. For both siRNAs, the mismatch sequences cloned in the same vector were used as experimental controls and were ineffective on NCX1 or NCX3 protein expression. After 15 hours of plating, PC-12 cells were transfected with pSUPER-NCX1, pSUPER-NCX3 or pSUPER-control by means of lipofectamine standard protocol. After 48 hours, cells were lysed and used to quantify NCX1 or NCX3 protein expression or treated with NGF for 7 days.

3.4 Generation and stable expression of wild-type, mutant, and chimeric NCX

Dog heart NCX1.1 and rat brain NCX3.3 cDNAs, both generous gifts from Dr. K. Philipson (UCLA, Los Angeles, California, USA), were cloned into pcDNA3.1 expression vector. NCX3 mutants were generated by means of QuikChange site-directed mutagenesis kit (Stratagene, Italy). Briefly, NCX3Δf mutant was obtained by removing the amino acid region 292-708 from $NCX3_{WT}$; $NCX3_{KK370WW}$ was obtained by replacing the amino acids lysin^{370} and lysin^{371} with tryptophan^{370} and tryptophan^{371}; N-NCX3 was generated by site-directed mutagenesis of the amino acids lysin^{371}, histidin^{372} and alanin^{373} in a triple stop codon; C-NCX3 was generated by cloning the amino acid region 513-927 of $NCX3_{WT}$ cDNA in the expression vector pEGFP-C2 (Clontech, USA). All mutants were verified by whole sequencing on both DNA strands (Primm, Milan, Italy). NCX1/NCX3 chimeras, cloned into pKCRH expressing vector, were a generous gift from Dr. T. Iwamoto (Fukuoka University, Fukuoka, Japan).

Wild-type, mutant, and chimeric exchangers were transfected in the BHK cell line by Lipofectamine 2000 (Invitrogen, Italy) following the manufacturer's instructions. Stable cell lines were selected by G418 resistance and by a Ca^{2+}-killing procedure.

3.5 **Electrophysiology**

NCX currents were recorded from primary hippocampal mouse neurons**,** NGF-differentiated PC-12**,** and BHK cells at 20–22℃ by the patch-clamp technique in whole-cell configuration using a commercially available amplifier and Digidata 1322A interface (Molecular Devices, Sunnyvale, CA) as previously described (Molinaro et al. 2008; He et al. 2003). NCX currents were recorded starting from a holding potential of –60 mV up to a short-step depolarization at +60 mV (60 ms). Then, a descending voltage ramp from +60 mV to –120 mV was applied. The current recorded in the descending portion of the ramp (from +60 mV to –120 mV) was used to plot the current–voltage (*I–V*) relation curve. The magnitude of I_{NCX} was measured at the end of +60 mV (reverse mode) and at the end of –120 mV (forward mode), respectively. The Ni^{2+}-insensitive component was subtracted from total currents to isolate I_{NCX}. In addition, the potassium, sodium and calcium currents were abolished by means of 20mM tetraethylammonium (TEA), 50 nM tetrodotoxin (TTX), and 10 μM nimodipine.

The neurons were perfused with external Ringer's solution containing the following (in mM): 126 NaCl, 1.2 $NaHPO_4$, 2.4 KCl, 2.4 $CaCl_2$, 1.2 $MgCl_2$, 10 glucose, and 18 $NaHCO_3$, pH 7.4. 20 mM TEA, 50nM TTX, and 10μM nimodipine were added to Ringer's solution. The dialyzing pipette solution contained the following (in mM): 100 K-gluconate, 10 TEA, 20 NaCl, 1 Mg-ATP, 0.1 $CaCl_2$, 2 $MgCl_2$, 0.75 EGTA, and 10 HEPES, adjusted to pH 7.2 with $Cs(OH)_2$. Possible changes in cell size occurring after specific treatments were calculated by monitoring the capacitance of each cell membrane, which is directly related to membrane surface area, and by expressing the current amplitude data as current densities (pA/pF). Capacitive currents were estimated from the decay of the capacitative transient induced by 5mV depolarizing pulses from a holding potential of –80mV and acquired at a sampling rate of 50kHz. The capacitance of the membrane was calculated according to the following equation: $C_m=\tau_c \cdot I_o/\Delta E_m(1-I_\infty/I_o)$, where C_m is the membrane capacitance, τ_c is the time constant of the membrane capacitance, I_o is the maximum capacitance current value, ΔE_m is the amplitude of the voltage step, and I_∞ is the amplitude of the steady-state current.

3.6 $[Ca^{2+}]_i$ measurement

$[Ca^{2+}]_i$ was measured by single cell computer-assisted videoimaging (Secondo et al. 2007). Briefly, primary hippocampal neurons, NGF-differentiated PC-12, and BHK cells, grown on glass coverslips, were loaded with 10µM Fura-2 acetoxymethyl ester (Fura-2AM) (Calbiochem, San Diego, CA, USA) for 30 minutes at 37°C. At the end of the Fura-2AM loading period, the coverslips were placed into a perfusion chamber (Medical System, Co. Greenvale, NY, USA) mounted onto a Zeiss Axiovert 200 microscope (Carl Zeiss, Germany) equipped with a FLUAR 40X oil objective lens. The experiments were carried out with a digital imaging system composed of MicroMax 512BFT cooled CCD camera (Princeton Instruments, Trenton, NJ, USA), LAMBDA 10-2 filter wheeler (Sutter Instruments, Novato, CA, USA), and Meta-Morph/MetaFluor Imaging System software (Universal Imaging, West Chester, PA, USA). After loading, cells were alternatively illuminated at wavelengths of 340 nm and 380 nm by a Xenon lamp. The emitted light was passed through a 512 nm barrier filter. Fura-2AM fluorescence intensity was measured every 3 seconds. Ratiometric values were automatically converted by the software into $[Ca^{2+}]_i$ using a preloaded calibration curve obtained in preliminary experiments as previously reported (Grynkiewicz *et al*. 1985). NCX activity was evaluated as Ca^{2+} uptake through the reverse mode by switching the normal Krebs medium to Na^+-deficient $NMDG^+$ medium (Na^+-free) (in mM): 5.5 KCl, 147 *N*-methyl glucamine, 1.2 $MgCl_2$, 1.5 $CaCl_2$, 10 glucose, and 10 Hepes–NaOH (pH 7.4). In the experiments involving the use of the irreversible and selective inhibitor of the ER Ca^{2+} ATPase (SERCA) thapsigargin (Tg) (1µM), this compound was added to the medium 10 minutes before the beginning of the recordings, as previously described (Secondo *et al* 2007). NCX activity was calculated as Δ% of peak/basal $[Ca^{2+}]_i$ values after the perfusion with a Na^+-free medium.

3.7 Assessment of nuclear morphology

Nuclear morphology was evaluated by using the fluorescent DNA-binding dye Hoechst-33258. To this aim, cells were fixed in 4% paraformaldehyde and incubated

for 5 minutes in PBS containing 1μg/ml Hoechst-33258 at 37°C. Coverslips were mounted on glass slides and observed with the fluorescence microscope Nikon Eclipse E400 (Nikon, Torrance, CA, USA). Digital images were taken with a CoolSNAP camera (Media Cybernetics Inc, Silver Spring, MD, USA), stored on the hard-disk of a Pentium III computer, and analyzed with the Image-Pro Plus 4.5 software (Media Cybernetics Inc, Silver Spring, MD, USA). Pathological nuclei were characterized by chromatin condensation (pyknosis) and fragmentation, or by decreases and increases in size (Pannaccione *et al*. 2005).

3.8 Western-blot analysis

After treatment, cells were lysed with a buffer containing 20mM Tris–HCl (pH 7.5), 10mM NaF, 1mM phenylmethylsulfonyl fluoride, 1% NONIDET P-40, 1mM Na_3VO_4, 0.1% aprotinin, 0.7 mg/ml pepstatin and 1μg/ml leupeptin. Samples were cleared by centrifugation and supernatants were used for Western blot. Protein concentration in supernatants was determined by Bradford method (Bradford, 1976). Protein samples (50μg) were analyzed on 8% sodium dodecyl sulfate polyacrilamide gel with 5% sodium dodecyl sulfate stacking gel (SDS-PAGE) and electrotransferred onto Hybond ECL nitrocellulose paper (Amersham). Membranes were blocked with 5% nonfat dry milk in 0.1% Tween 20 (TBS-T; 2 mmol/l Tris–HCl, 50 mmol/l NaCl, pH 7.5) for 2 h at RT and subsequently incubated overnight at 4 °C in the blocked buffer with the antibody for NCX1, NCX3, caspase-12, calpain.

The membranes were washed with 0.1% Tween 20 and incubated with the secondary antibodies (1:1000; Amersham) for 1 h. Immunoreactive bands were detected with the ECL (Amersham). The optical density of the bands (normalized with those of actin) was determined by Chemi Doc Imaging System (Biorad).

3.9 Statistical analysis

Statistical comparisons between controls and treated experimental groups were performed by ANOVA followed by Newman test or Student t test. Differences were considered to be statistically significant when p values were <0.05.

4. RESULTS

4.1 Effect of $A\beta_{1-42}$ fragment on NCX activity in hippocampal neurons and NGF-differentiated PC-12 cells

After $A\beta_{1-42}$ exposure, NCX currents in both hippocampal and NGF-differentiated PC-12 cells were assessed in the reverse and forward modes of operation by patch clamp in a whole-cell configuration.

$A\beta_{1-42}$ induced a significant concentration-dependent (Fig. 4A) increase only in NCX currents operating in the reverse mode, whereas it was ineffective in currents operating in the forward mode (Fig. 4A-E). Consistently, as revealed by Fura-2AM microfluorimetry, NCX activity in the reverse mode of operation was significantly increased in hippocampal neurons and in NGF-differentiated PC-12 cells treated with 5 μM $A\beta_{1-42}$ for 24 hours (Fig. 4F and 4G).

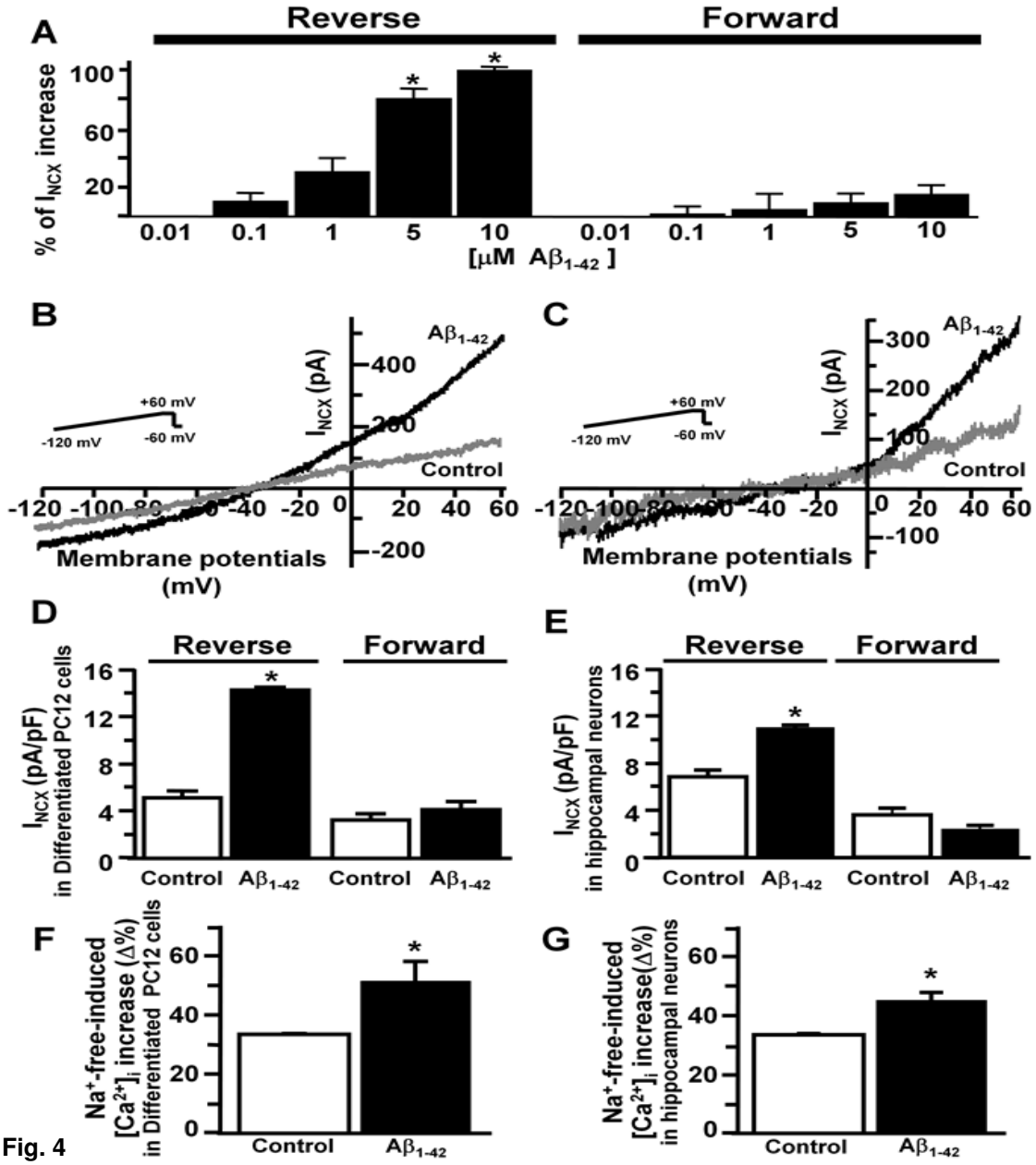

Fig. 4

Fig. 4 Effect of $A\beta_{1-42}$ fragment on NCX activity in hippocampal neurons and NGF differentiated PC 12 cells. (A) Quantification of $A\beta_{1-42}$ dose-dependent (0.01-10μM) effect on I_{NCX} in the reverse and forward modes of operation. **(B)** and **(C)** I_{NCX} superimposed traces recorded under control conditions (gray trace) and after 24 hours of 5μM $A\beta_{1-42}$ (black trace) in NGF-differentiated PC12 cells and in primary hippocampal neurons, respectively. **(D)** and **(E)** Quantification of I_{NCX} represented in **B** and **C** panels, respectively. **(F)** and **(G)** Quantification of NCX activity in the reverse mode of operation elicited by Na^+-free perfusion under control conditions and after exposure to $A\beta_{1-42}$ (5μM, 24 hours) recorded in hippocampal neurons and NGF-differentiated PC12 cells, respectively. All the values are expressed as mean ±SEM of current densities (n= 20 cells in 3 independent experimental sessions). **p*<0.05 versus their respective controls.

4.2 Effect of NCX3 silencing or knocking-out on $A\beta_{1-42}$-induced upregulation of NCX currents

Patch clamp experiments showed that the silencing of NCX3, but not of NCX1, prevented the $A\beta_{1-42}$-induced upregulation in I_{NCX} in the reverse mode of operation in NGF-differentiated PC-12 cells (Fig. 5A-C). Accordingly, $A\beta_{1-42}$ treatment failed to increase the NCX currents in primary hippocampal neurons obtained from *ncx3-/-* mice (Fig. 5D).

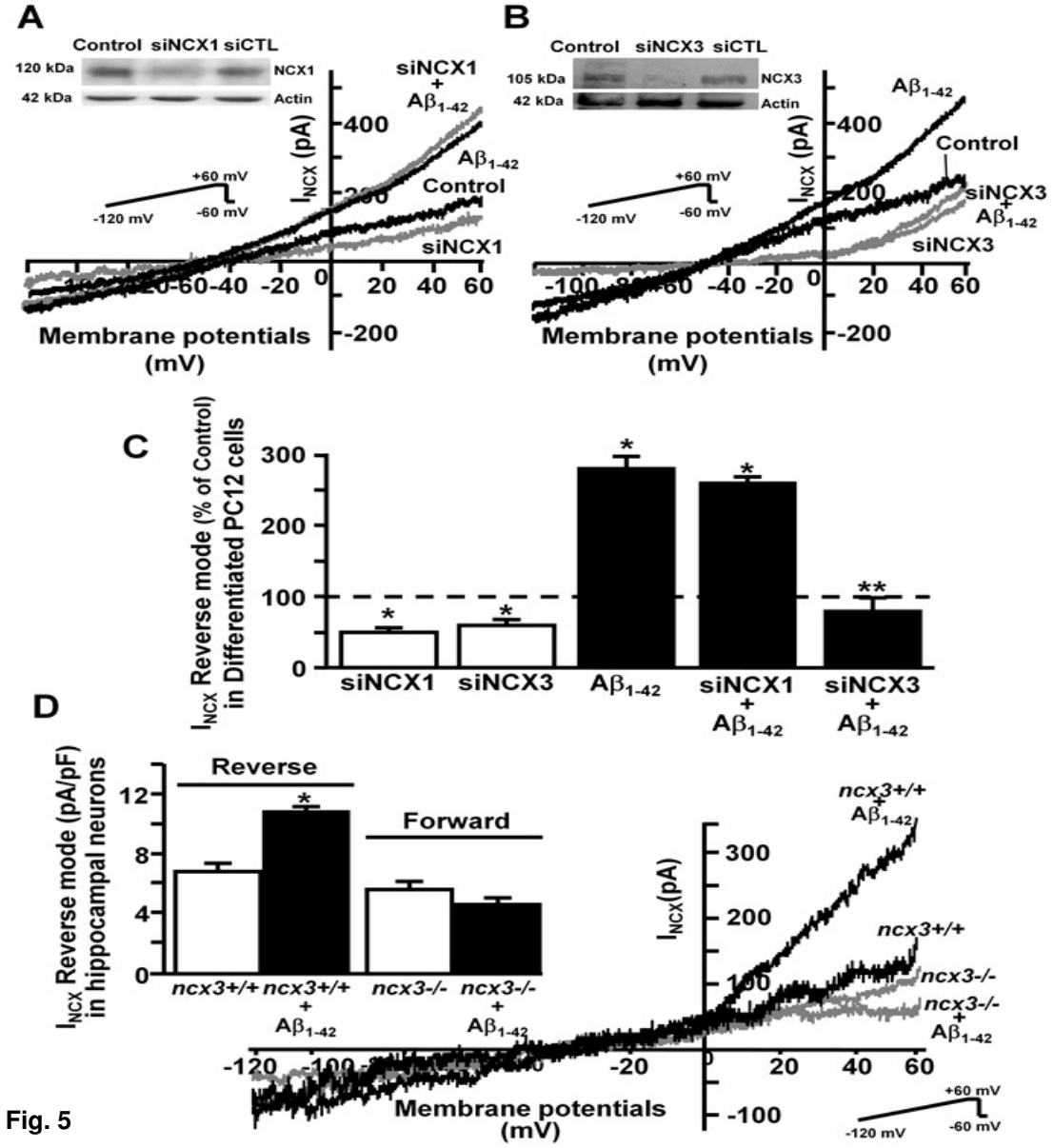

Fig. 5

Fig. 5 Effect of NCX3 silencing or knocking-out on Aβ$_{1-42}$-induced upregulation of NCX currents in hippocampal neurons and NGF-differentiated PC-12 cells.

(A) Representative western blot of NCX1 silencing (upper panel **A**), and I_{NCX} superimposed traces recorded from control (black trace), control plus siNCX1 (gray trace), after 5μM Aβ$_{1-42}$ for 24 hours (black trace), and after 5μM Aβ$_{1-42}$ for 24 hours plus siNCX1 (gray trace) in NGF-differentiated PC12 cells. **(B)** Representative western blot of siNCX3 on protein expression (upper panel **B**), and I_{NCX} under the same experimental conditions of panel A. **(C)** Quantification of I_{NCX} represented in panels **A** and **B**. **(D)** I_{NCX} superimposed traces recorded from *ncx3+/+* and *ncx3-/-* primary hippocampal neurons under control conditions and after 24 hours of Aβ$_{1-42}$ exposure. Inset depicts the quantification of I_{NCX}. All the values are expressed as mean±SEM of current densities (n= 20 cells in 3 independent experimental sessions). **p*<0.05 versus their respective controls; **p<0.05 versus Aβ$_{1-42}$.

4.3 Effect of $A\beta_{1-42}$ on calpain activation and on the formation of the NCX3 proteolytic fragment

Immunoblot analysis performed on NGF-differentiated PC-12 cells revealed two bands at ~105 and ~75 kDa corresponding to the native and proteolytic bands of NCX3, respectively, in both control and $A\beta_{1-42}$-treated groups (Fig. 6A). Densitometric analysis showed that the native band at ~ 105 kDa decreased in $A\beta_{1-42}$-treated cells than in controls, whereas the ~ 75 kDa proteolytic band was significantly increased (Fig. 6A). Interestingly, exposure to 5 μM $A\beta_{1-42}$ caused an increase in $[Ca^{2+}]_i$ at 30 minutes (Fig. 6B), which was accompanied by calpain activation lasting 3 hours (Fig. 6C). The selective calpain inhibitor calpeptin (100 nM) prevented both the $A\beta_{1-42}$-induced generation of the ~75 kDa proteolytic fragment (Fig. 6D) and the increase in I_{NCX3} in the reverse mode of operation (Fig. 6E). Accordingly, in BHK cells stably transfected with NCX3, 5 μM $A\beta_{1-42}$ induced an increase in $[Ca^{2+}]_i$ at 6 and 12 hours (Fig. 7A). This $[Ca^{2+}]_i$ increase was accompanied by the activation of calpain at 6 and 12 hours (Fig. 7B). Moreover, immunoblot analysis revealed a significant increase in the ~55 kDa band (the proteolytic band in the BHK cells has a different weight respect than in the neuronal cells) in $A\beta_{1-42}$-treated BHK-NCX3 cells and a significant reduction in the NCX3 native band at ~105 kDa (Fig. 7C). In addition, in BHK-NCX3 cells $A\beta_{1-42}$ fragment (5 μM for 24 hours) induced an increase in NCX currents in the reverse mode of operation (Fig. 7D).

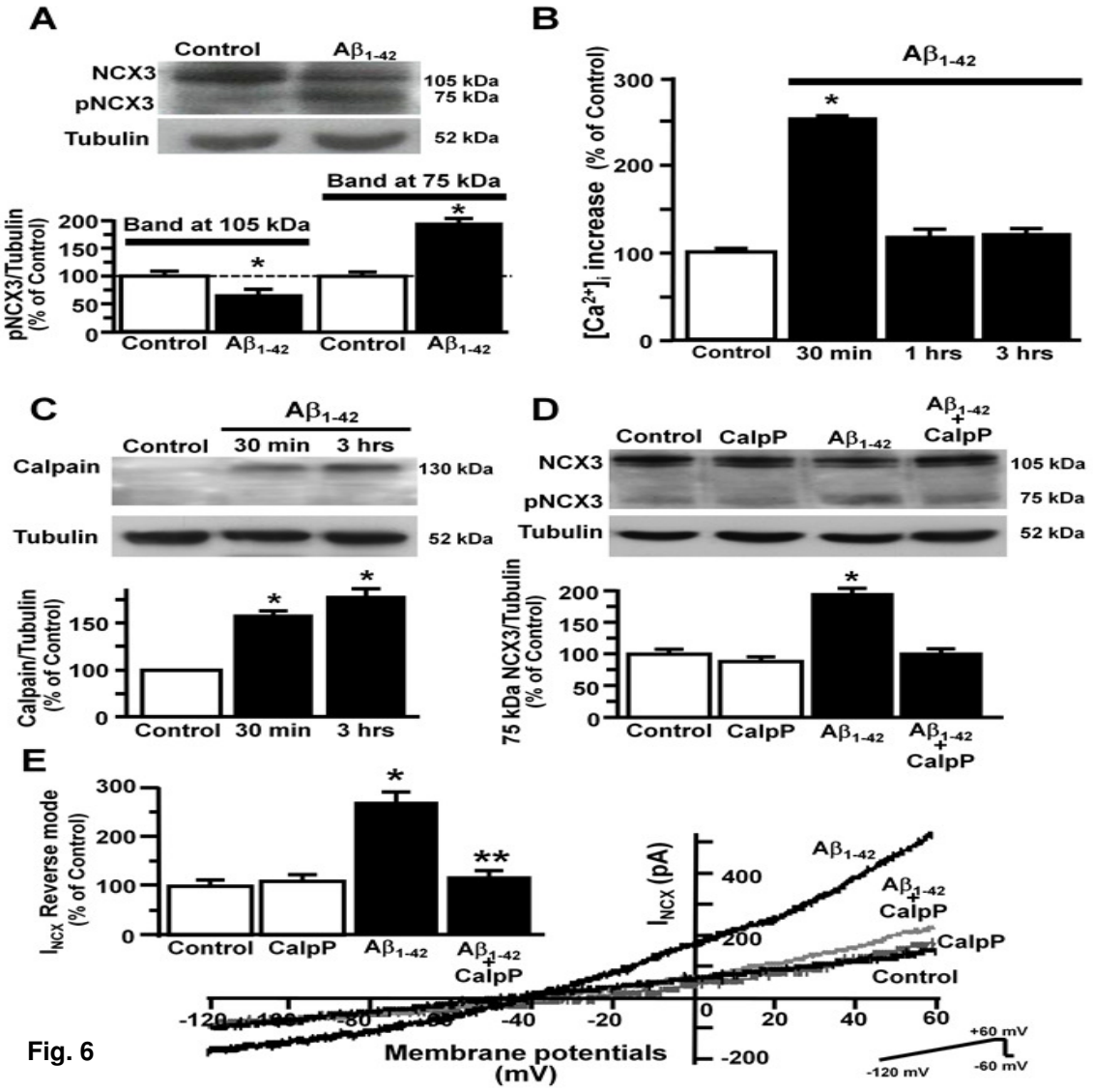

Fig. 6

Fig. 6 Effect of Aβ_{1-42} on calpain activation and on the formation of NCX3 proteolytic fragments in NGF-differentiated PC-12 cells. (A) Representative western blot and densitometric quantification of NCX3 expression under control conditions and after 24 hours of Aβ_{1-42}. (**B**) Quantification of the time-dependent effect of Aβ_{1-42} on $[Ca^{2+}]_i$. (**C**) Representative western blot and densitometric quantification of calpain activation under control conditions, after 30 minutes and 3 hours of Aβ_{1-42} exposure. (**D**) Representative western blot and densitometric quantification of NCX3 expression in the presence and in the absence of calpeptin (CalpP) in control conditions and after Aβ_{1-42} exposure. (**E**) I_{NCX} superimposed traces recorded in the presence and in the absence of CalpP in control conditions and after Aβ_{1-42} exposure. Inset depicts the quantification of I_{NCX}. The values are expressed as mean±SEM of 3 independent experimental sections. *p<0.05 versus their respective controls; **p<0.05 versus Aβ_{1-42}.

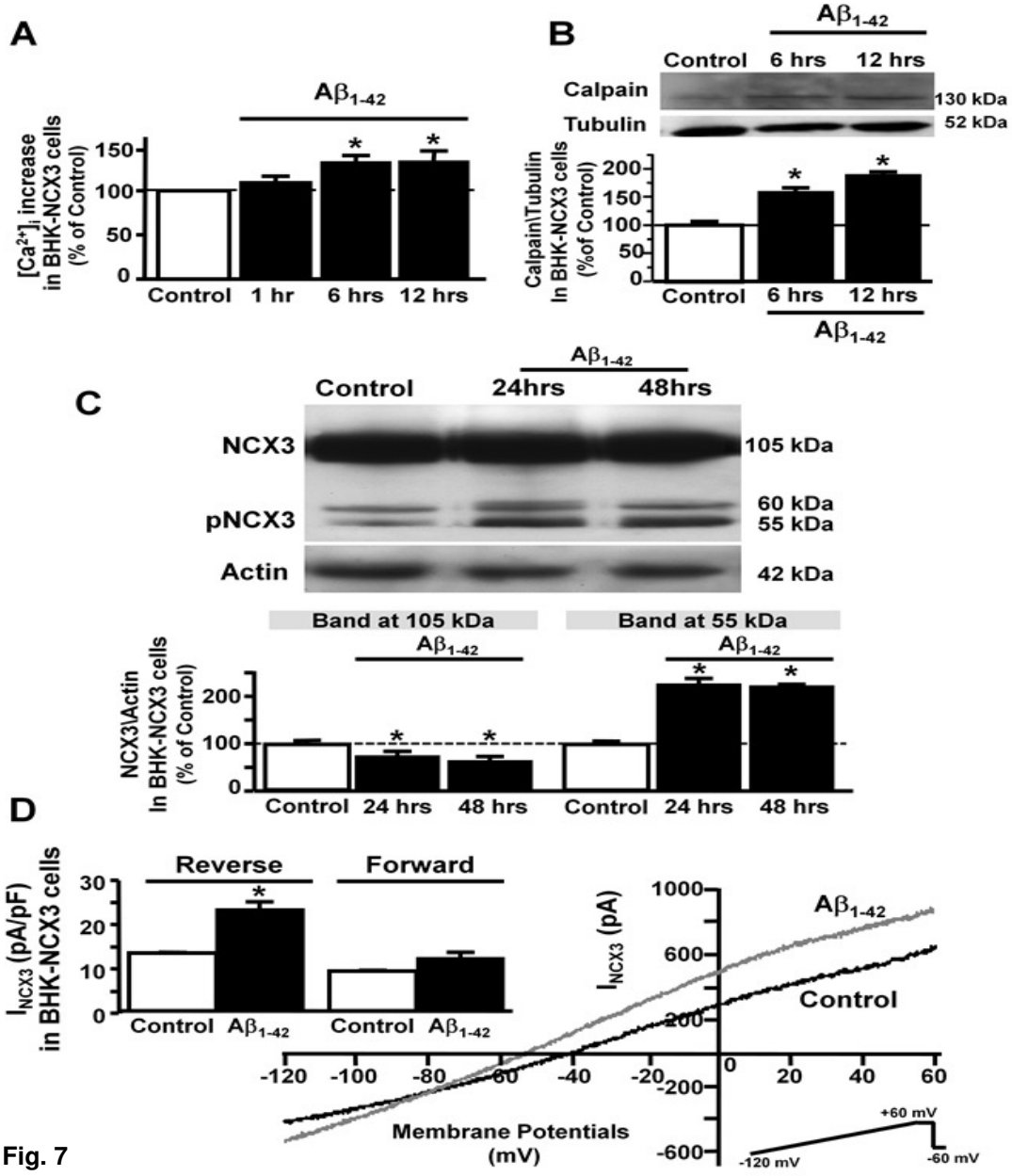

Fig. 7

Fig. 7 Effect of $A\beta_{1-42}$ on calpain activation and on the formation of NCX3 proteolytic fragments in stably transfected BHK-NCX3 cells. (A) Quantification of the time-dependent effect of $A\beta_{1-42}$ on $[Ca^{2+}]_i$. (**B**) Representative western blots and densitometric quantification of calpain activation under control conditions and after 6 and 12 hours of $A\beta_{1-42}$ exposure. (**C**) Representative western blot and densitometric quantification of NCX3 expression under control conditions and after 24 and 48 hours of $A\beta_{1-42}$ exposure. (**D**) Superimposed traces of I_{NCX3} recorded in control conditions and after $A\beta_{1-42}$ exposure. Inset depicts the quantification of I_{NCX3}. The values are expressed as mean±SEM of 3 independent experimental sections. **p*<0.05 versus their respective controls.

4.4 Effects of $A\beta_{1-42}$ on NCX currents in BHK cells stably transfected with NCX3 mutant and chimeras

To investigate the molecular determinants of calpain-dependent effects of $A\beta_{1-42}$ on NCX3 activity, the region containing calpain cleavage sites (Fig. 8A) and belonging to the transmembrane segment TM5 and to a part of the cytoplasmic f-loop, (227-469), named $NCX3_{NCX1TM5}$, was substituted with the homologous region of NCX1, which is insensitive to $A\beta_{1-42}$-induced calpain cleavage.

Vice versa, the sensitive NCX3 TM5 f-loop region was replaced with the homologous insensitive region of NCX1, named $NCX1_{NCX3TM5}$.

The mutant, named NCX3Δf, was obtained by removing the large f-loop in NCX3 cDNA. All these chimeras and the mutant, stably transfected in BHK cells, were able to generate NCX currents similar to those carried by wild-type NCX1 and NCX3 (Fig. 9).

Patch-clamp experiments revealed that the substitution of NCX3 TM5 f-loop ($NCX3_{NCX1TM5}$) or the removal of the f-loop (NCX3Δf) prevented the stimulatory effect of $A\beta_{1-42}$ on NCX currents (Fig. 8B).

By contrast, the activity of the reverse chimera of $NCX3_{NCX1TM5,}$ named $NCX1_{NCX3TM5}$, was inhibited by $A\beta_{1-42}$ exposure (Fig. 8B). In addition, the activity of $NCX3_{NCX1TM6}$, which contains the calpain cleavage sites, was increased after $A\beta_{1-42}$ exposure in the reverse mode of operation (Fig. 8B).

Immunoblot experiments revealed that all NCX3 chimeras were recognized by the NCX3 antibody raised against the large intracellular f-loop (Fig. 8C, and 8D). Interestingly, $A\beta_{1-42}$ treatment upregulated the 55 kDa proteolytic band of the $NCX3_{NCX1TM6}$ chimera containing the calpain cleavage site (Fig. 8C), whereas it did not modify the intensity of the same band in $NCX3_{NCX1TM5}$ chimera lacking the calpain cleavage site (Fig. 8D).

Moreover, immunoblot analysis did not reveal any band in BHK-NCX3Δf mutant because this mutant lacked the antibody recognizing sites (data not shown). To investigate further the molecular determinants within the amino acid sequence 227-469 responsible for the $A\beta_{1-42}$-induced calpain-dependent effect on NCX3 current

upregulation, we performed a site-directed mutagenesis of two lysine residues (370-371) essential for calpain cleavage.

The mutant, named $NCX3_{KK/WW}$, lacking the calpain cleavage sequence, was not modulated by $A\beta_{1-42}$ in the reverse mode of operation (Fig. 10A-C).

In addition, western blot analysis of BHK cells expressing the $NCX3_{KK/WW}$ mutant did not reveal the band at 55 kDa either under control conditions or after $A\beta_{1-42}$ exposure (Fig. 10D).

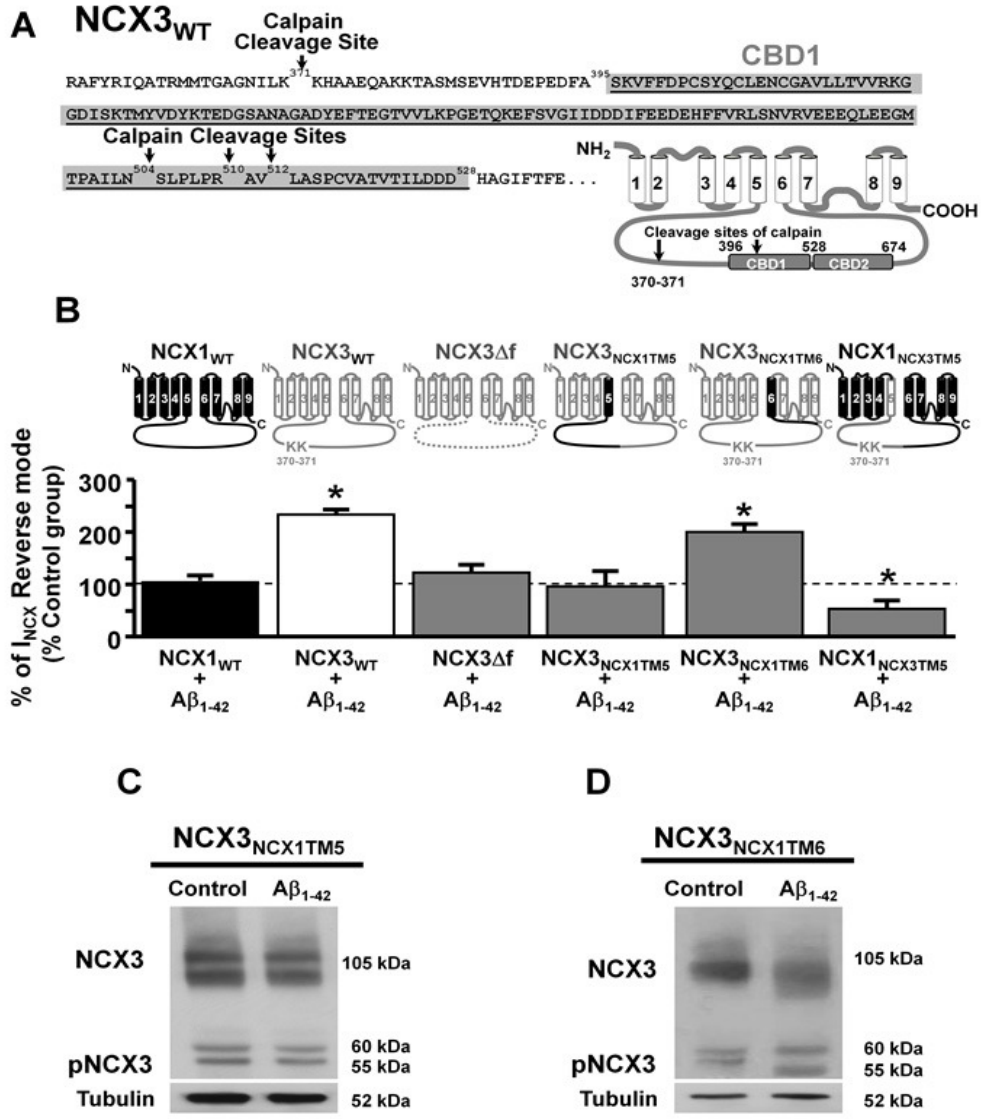

Fig. 8

Fig. 8 Effects of $A\beta_{1-42}$ on NCX currents in NCX3 mutant and chimeras in stably transfected BHK cells. (A) NCX3 sequence containing the calpain cleavage sites. (**B**) Quantification of the $A\beta_{1-42}$ effect on I_{NCX} recorded in BHK cells transfected with each single chimera and mutant. The values are expressed as mean±SEM of 3 independent experimental sections. *p<0.05 versus their respective controls. (**C**) Representative western blot of $NCX3_{NCX1TM5}$ expression in control conditions and after $A\beta_{1-42}$ exposure. (**D**) Representative western blot of $NCX3_{NCX1TM6}$ expression in control conditions and after $A\beta_{1-42}$ exposure.

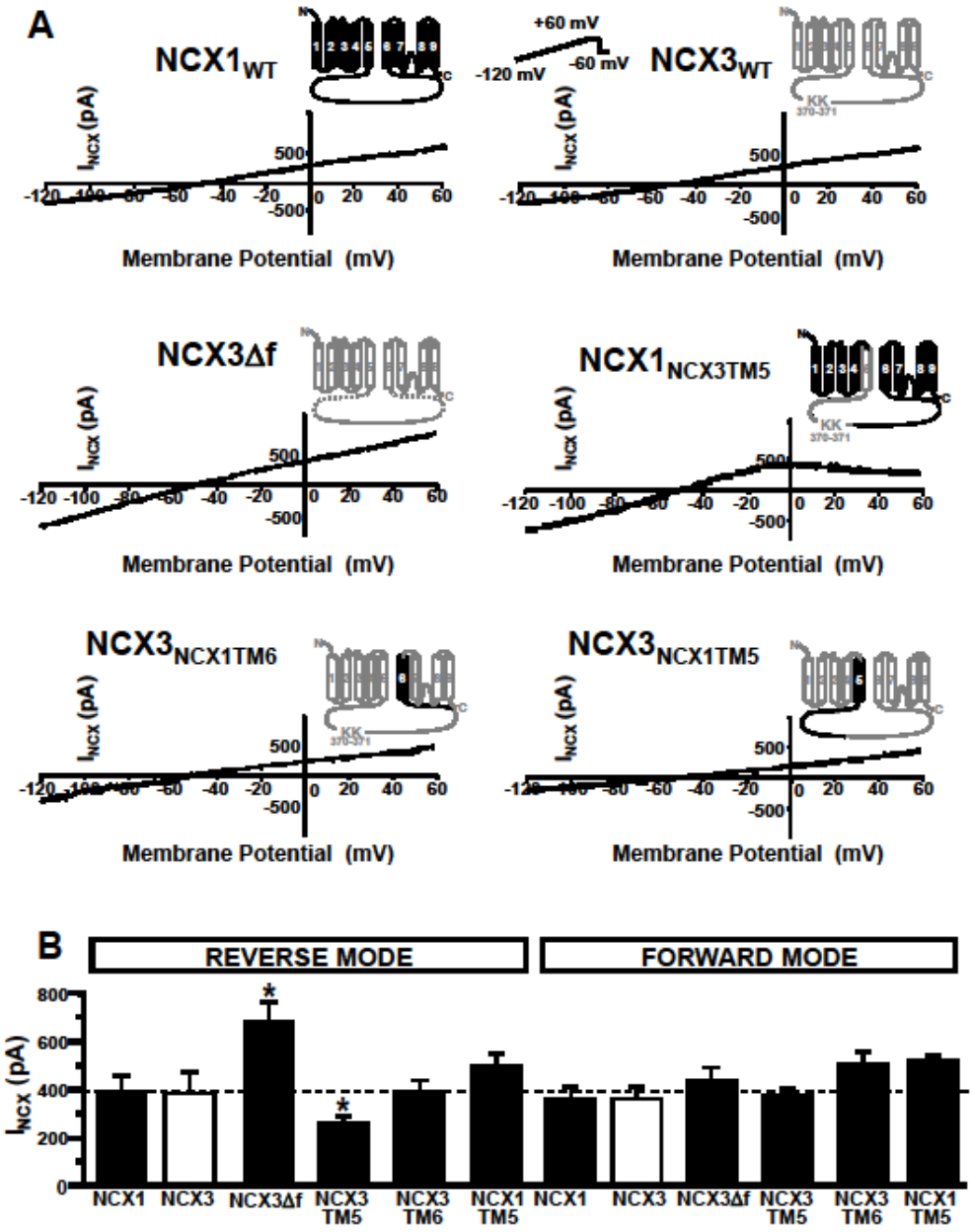

Fig. 9

Fig. 9 Electrophisiology activity of the NCX3 mutant and chimeras in stably transfected BHK cells.

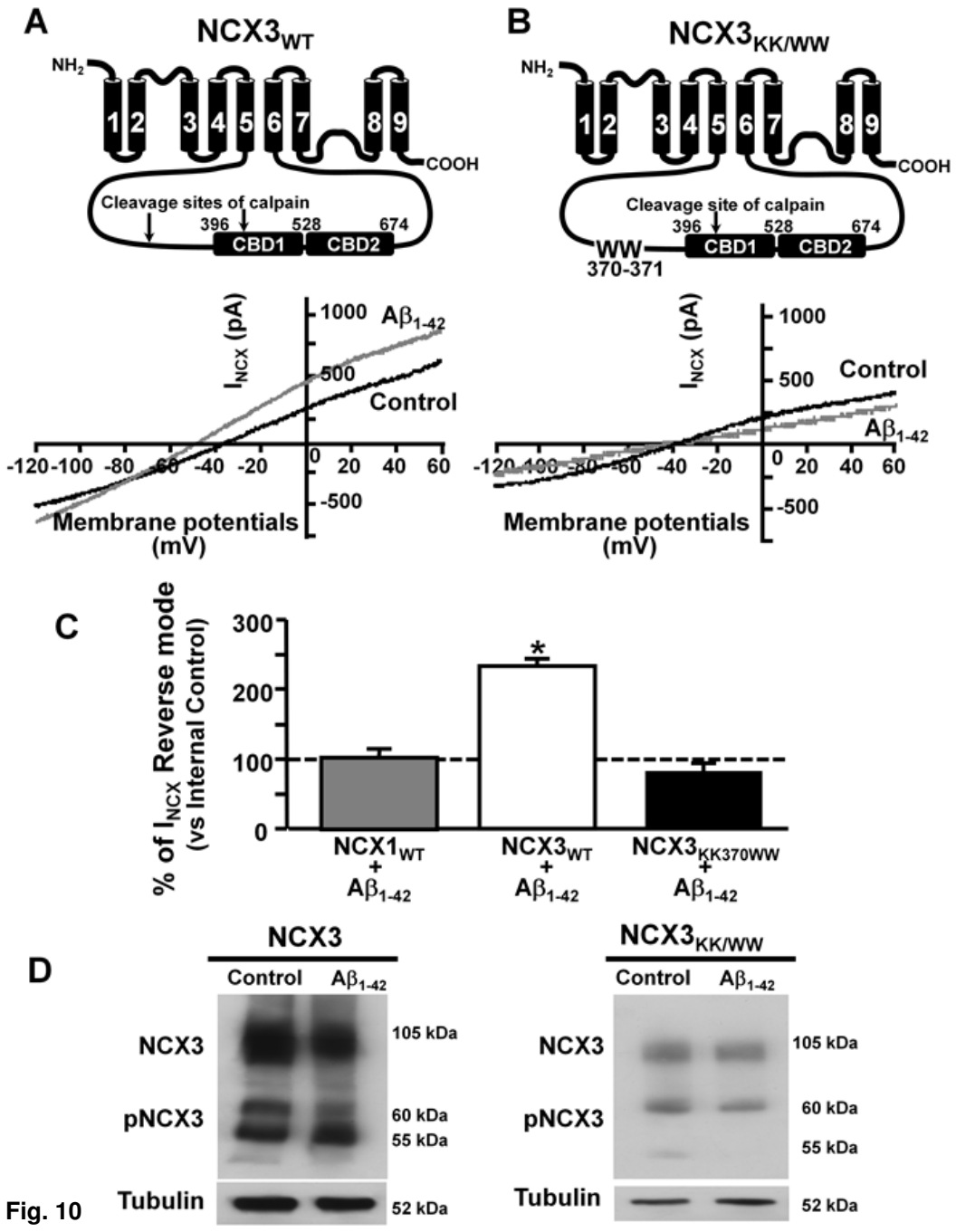

Fig. 10

Fig. 10 Effects of Aβ_{1-42} on NCX currents in NCX3$_{KK/WW}$ in stably transfected BHK cells.

(A) I_{NCX3} superimposed traces recorded in NCX3$_{WT}$ in control conditions and after Aβ_{1-42} exposure. (**B**) I_{NCX} superimposed traces recorded in transfected BHK cells with NCX3$_{KK/WW}$ in control conditions and after Aβ_{1-42}. **(C)** Quantification of the Aβ_{1-42} effect on I_{NCX} in the same experimental conditions of panels A and B. The values are expressed as mean±SEM of 3 independent experimental sections. *p<0.05 versus their respective controls. (**D**) Representative western blots of NCX3 and NCX3$_{KK/WW}$ expression in control conditions and after Aβ_{1-42} exposure.

4.5 Patch clamp analysis in BHK cells overexpressing the NH_2-terminal proteolytic fragment of NCX3

To characterize further the activity of the proteolytic fragments of NCX3 produced by $A\beta_{1-42}$-induced calpain cleavage, we made cDNA constructs encoding for both NH_2- and COOH- terminus halves of NCX3, named N-NCX3 and C-NCX3, respectively (Fig. 11A and 11B). Patch clamp recordings revealed that the N-NCX3 fragment carried currents comparable to those elicited by $A\beta_{1-42}$ treatment (5 μM, 24 hours) in BHK-NCX3 cells and greater than those recorded under control conditions (Fig. 11A and 11C). By contrast, C-NCX3 fragment did not carry significant currents (Fig. 11B and 11C).

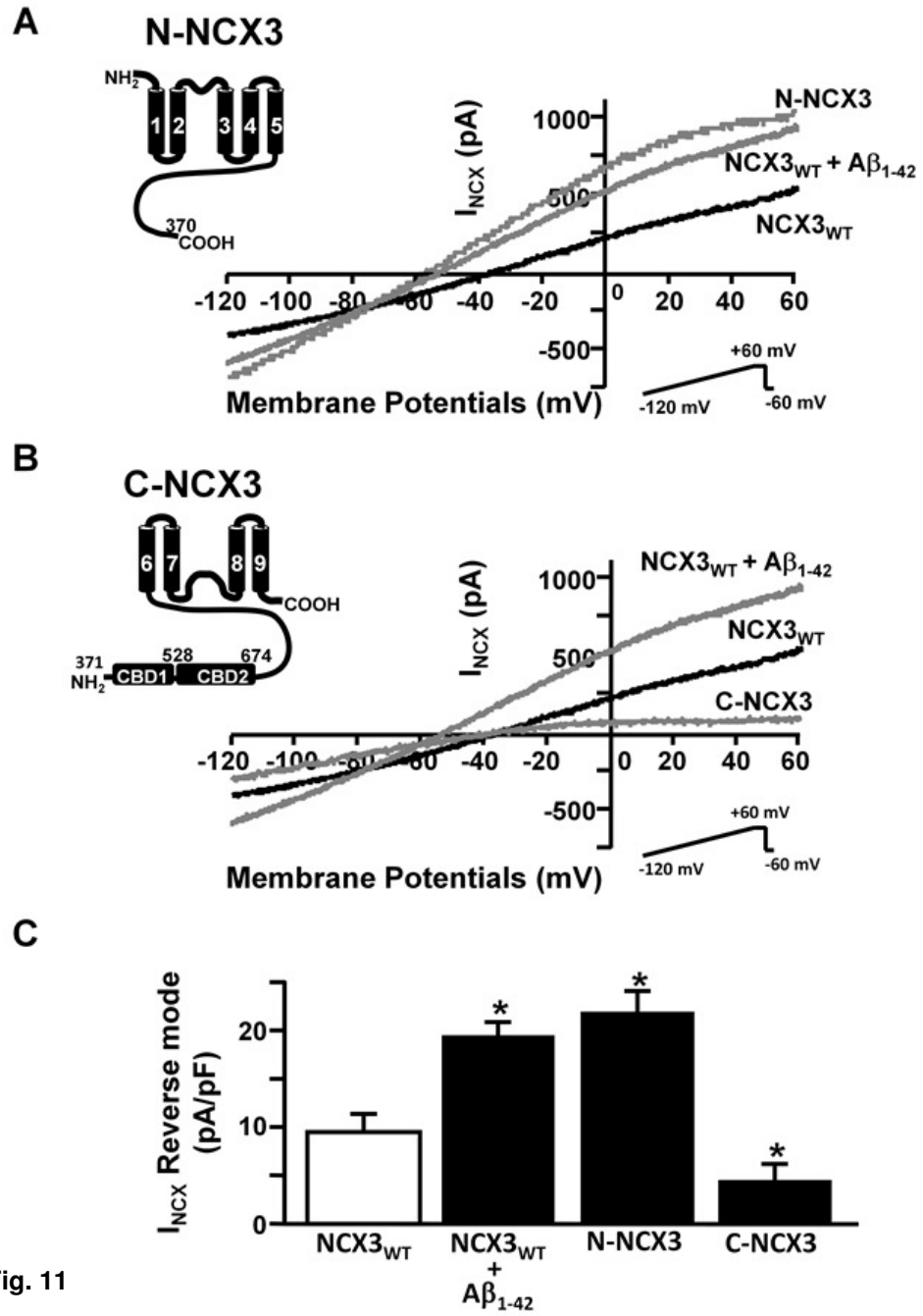

Fig. 11

Fig. 11 Patch clamp analysis in BHK cells overexpressing the NH_2-terminal proteolytic fragment of NCX3. (A) I_{NCX} superimposed traces recorded in BHK-NCX3 (black line) and in BHK-N-NCX3 (grey line) cell lines in control conditions and after exposure to $A\beta_{1-42}$ (grey line). (**B**) I_{NCX} superimposed traces recorded in BHK-NCX3 (black line) and in BHK-C-NCX3 (grey line) cells in control conditions and after $A\beta_{1-42}$ exposure (grey line). (**C**) Quantification of I_{NCX} expressed in A and B panels. The values are expressed as mean±SEM of 3 independent experimental sections. **p*<0.05 versus NCX3 wild-type.

4.6 Effect of *ncx3* silencing or knocking-out on Ca^{2+} refilling into ER induced by $A\beta_{1-42}$

After 24 hours of $A\beta_{1-42}$ exposure, the SERCA inhibitor thapsigargin induced a release of Ca^{2+} from ER stores higher than that obtained under control conditions in both hippocampal neurons and NGF-differentiated PC-12 cells, thus demonstrating that during $A\beta_{1-42}$ exposure, a larger Ca^{2+} accumulation occurs in ER (Fig. 12). This larger $A\beta_{1-42}$-induced ER-Ca^{2+} accumulation, however, was prevented when NCX3 was silenced or knocked-out (Fig. 12B-C), an event that suggested the important role of the increased activity of NCX3 in the ER-refilling process. Relevantly, the blockade of L-, N- and P/Q-type VDCC with their specific inhibitors nimodipine (10 μM), ϖ-conotoxin (200 nM), and ϖ-agatoxin (200 nM) did not prevent ER Ca^{2+} refilling induced by $A\beta_{1-42}$ exposure (data not shown).

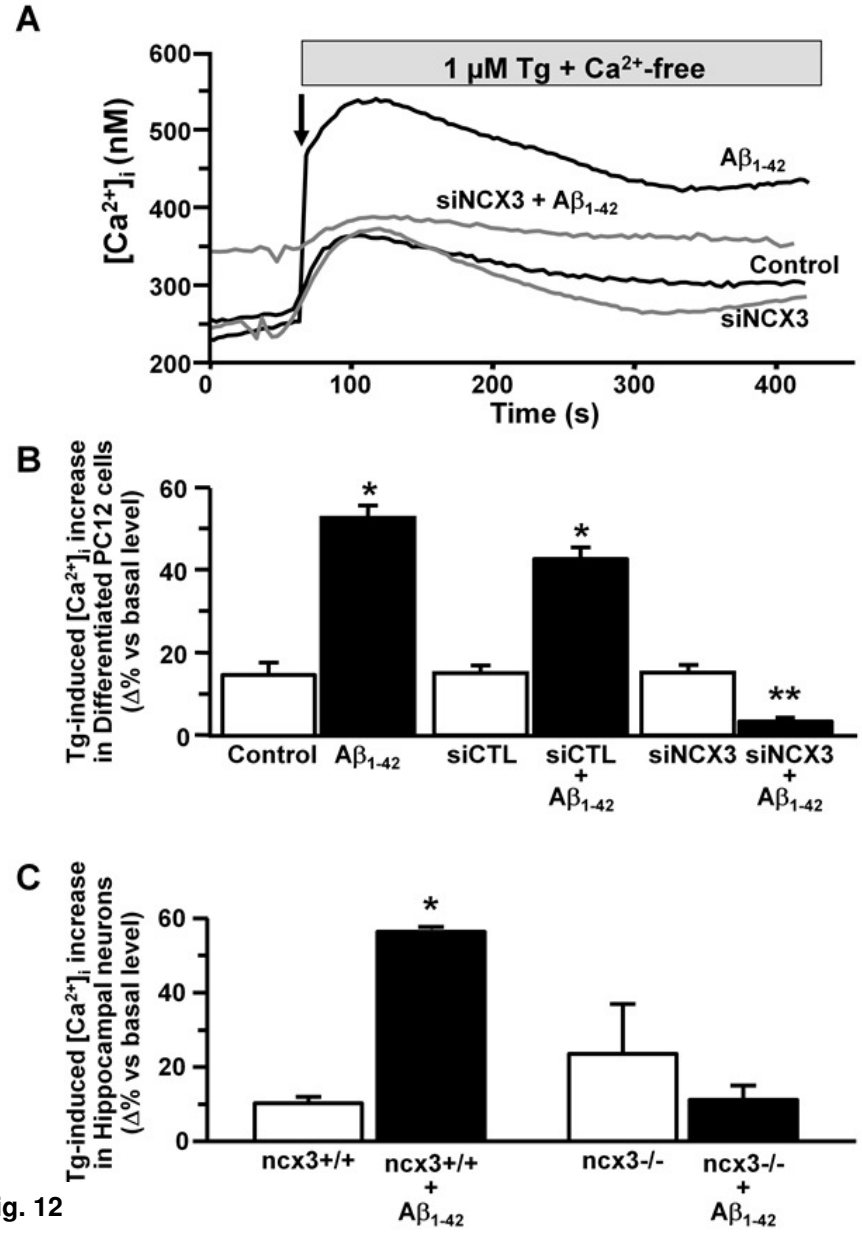

Fig. 12

Fig. 12 Effect of *ncx3* silencing or knocking-out on Ca^{2+} refilling into ER induced by $A\beta_{1-42}$. (**A**) Superimposed single-cell traces of the effect of thapsigargin (Tg; 1 µM) on $[Ca^{2+}]_i$ in Ca^{2+}-free (0 Ca^{2+}/1.5 mM EGTA) added to control (black trace), control plus siNCX3 (gray trace), after 24 hours $A\beta_{1-42}$ (black trace), and after 24 hours $A\beta_{1-42}$ plus siNCX3 (gray trace) in NGF-differentiated PC12 cells. (**B**) Quantification of Tg-induced $[Ca^{2+}]_i$ release in the experimental conditions of panel A. (**C**) Quantification of Tg-induced $[Ca^{2+}]_i$ release in *ncx3+/+* and *ncx3–/–* primary hippocampal neurons in control conditions and after 24 hours of $A\beta_{1-42}$ exposure. Each bar represents the mean±SEM (n=50 cells in 3 independent experimental sessions). **p*<0.05 versus their untreated controls; **p<0.05 versus its respective control and $A\beta_{1-42}$.

4.7 Effect of *ncx3* silencing on caspase-12 activation, neuronal apoptosis and death induced by $A\beta_{1-42}$ in NGF-differentiated PC-12 cells

After 72 hours of $A\beta_{1-42}$ exposure, caspase-12, a specific marker of ER stress, was activated in NGF-differentiated PC-12 cells (Fig. 13A). Interestingly, when NCX3 activity was silenced by siRNA, $A\beta_{1-42}$-induced caspase-12 activation occurred 48 hours earlier (Fig. 13B). Consistently, NCX3 silencing in $A\beta_{1-42}$-treated neuronal cells hastened and enhanced the appearance of abnormal nuclear morphology, as detected by Hoechst-33258 (Fig. 13C). Furthermore, neuronal cell death, monitored by propidium iodide, was reinforced by NCX3 silencing in $A\beta_{1-42}$-treated neuronal cells (Fig. 13D).

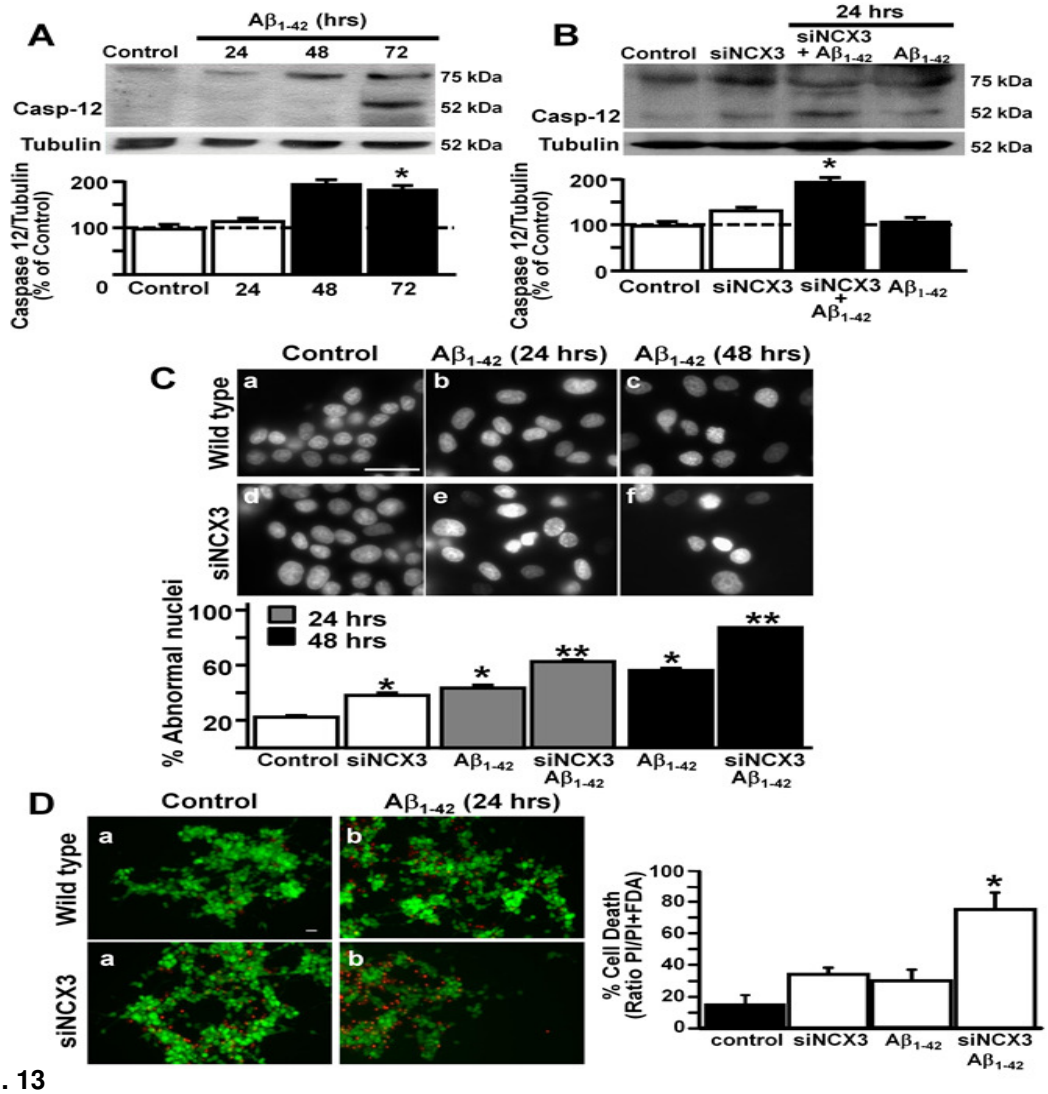

Fig. 13

Fig. 13 Effect of *ncx3* silencing on caspase-12 activation and neuronal apoptosis and death induced by $A\beta_{1\text{-}42}$ in NGF-differentiated PC-12 cells. (A) Representative western blot and densitometric quantification of the time-dependent effect of $A\beta_{1\text{-}42}$ on caspase-12 activation in control conditions. (**B**) Representative western blot and its densitometric quantification of caspase-12 activation in the presence and in the absence of siNCX3 and after 24 hours of $A\beta_{1\text{-}42}$ exposure in the presence and in the absence of siNCX3. All the data are expressed as means±SEM (n=5) and normalized on the basis of tubulin levels. (**C**) Assessment of nuclear morphology with Hoechst-33258 in NGF-differentiated PC-12 cells under control conditions in the presence and in the absence of siNCX3 and after 24 and 48 hours of $A\beta_{1\text{–}42}$ in the presence and in the absence of siNCX3. The quantification of the results was obtained in 4 separate experiments in which at least 10 microscopic fields were analyzed (~ 1000 cells per group). Scale bar 50 μm. **p*<0.05 versus controls; ***p*<0.05 versus $A\beta_{1\text{–}42}$ groups. (**D**) Cell death detected under the previously mentioned conditions in NGF-

differentiated PC-12 cells and represented as percentage of the ratio between PIpositive and PI+fluoresceinpositive cells. Scale bar 20 µm. *p<0.05 versus all.

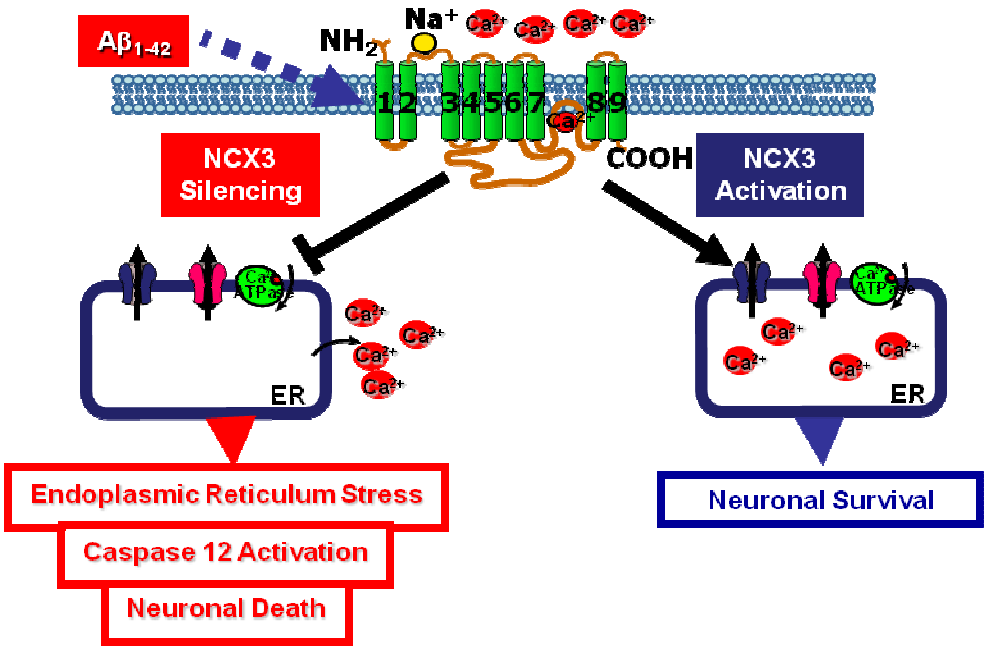

Fig. 14 $A\beta_{1-42}$ pattern hypothesis on NCX3

5. DISCUSSION

The results of the present thesis demonstrated for the first time that, in neurons, $A\beta_{1-42}$ peptide induces a dose-dependent increase in NCX currents in the reverse mode of operation and that this increase is mediated by the NCX3 isoform. Indeed, this augmented activity was due to the increased formation of a hyperfunctional proteolytic fragment of NCX3, induced by Ca^{2+}-dependent calpain activation. In fact, the removal of the consensus site for calpain cleavage located on the f-loop prevented the formation of the proteolytic fragment and abolished the stimulatory effect of $A\beta_{1-42}$ on NCX3 currents. Accordingly, the expression of the calpain-induced N-terminal proteolytic fragment of NCX3 in stably transfected cells carried NCX currents that were comparable to those recorded in control BHK-NCX3 cells exposed to $A\beta_{1-42}$. Moreover, this proteolytic fragment contributed to Ca^{2+} refilling into the ER by delaying ER stress. These data suggest that the formation of the hyperfunctional proteolytic fragment of NCX3 might represent a neuroprotective mechanism during $A\beta_{1-42}$ insult, for it helps neurons to delay ER stress, caspase-12 activation, apoptosis, and neuronal death.

It is well known that $A\beta_{1-42}$ exposure induces an increase in $[Ca^{2+}]_i$ either by functioning as a channel *per se* or by activating other Ca^{2+} channels. This increase, in turn, triggers a Ca^{2+}-dependent calpain activation in AD and other neurodegenerative diseases (Vosler *et al.*,2008). On the other hand, NCX3 sequence contains, at the level of the f-loop, two calpain cleavage sites (Bano *et al.* 2005). In the present study, we found that the two lysine residues (370-371) in the f-loop of the NCX3 sequence may represent the molecular determinants of calpain cleavage and are therefore responsible for the $A\beta_{1-42}$ stimulatory effect on NCX3. In fact, when the two lysine residues are replaced with two tryptophan residues, that are not recognized by calpain (Tompa *et al.* 2004), the formation of the hyperfunctional proteolytic fragment is repressed. Another study has shown that during brain ischemia and glutamate exposure, NCX3 can be cleaved by the Ca^{2+}-activated calpain at the same consensus sites, thus producing similar proteolytic fragments (Bano *et al.* 2005). This mechanism has been interpreted as a destruction of the cellular defences following

stroke (Choi 2005). By contrast, in our study we demonstrated that this cleavage produced a hyperfunctional proteolytic fragment of NCX3 that, in the early phases of $A\beta_{1-42}$ exposure, helps neurons to maintain the $[Ca^{2+}]_i$ homeostasis, thus delaying by 48 hours the activation of caspase-12. This hypothesis was further reinforced by the results showing that the silencing of NCX3 accelerated caspase-12 activation and neuronal death. On the other hand, this NCX3 neuroprotective role during the initial phase of $A\beta_{1-42}$ exposure resembles that observed in our laboratory during brain ischemia in rats (Pignataro *et al.* 2004), in *ncx3* knock-out mice (Molinaro *et al.* 2008), and in an *in vitro* model of OGD (Secondo *et al.* 2007).

The first step in the chain of events triggered by $A\beta_{1-42}$ exposure seems to be the Ca^{2+}-dependent formation of a terminal proteolytic fragment of NCX3 responsible for the increase in NCX3 activity. Indeed, our results revealed that the transfection of cDNA encoding for the N-terminal proteolytic fragment of NCX3 in BHK wild type cells carried NCX currents that were comparable to those recorded after $A\beta_{1-42}$ exposure. Interestingly, two previous studies have reported that the expression of the N-terminal half of the exchanger can by itself induce NCX activity, suggesting that the truncated exchanger can dimerize and form a functional exchanger (Gabellini *et al.*, 1996; Li and Lytton, 1999). Interestingly, several years ago, Colvin *et al.* (1994; 1997) observed an increase in NCX activity in plasma membrane vesicles from human *post mortem* tissues of frontal cortex, temporal cortex and cerebellum of AD patients.

Moreover, the increased activity of the proteolytic fragment of NCX3 may occurr in the ER refilling dysregulation observed in AD and in other neurodegenerative diseases. In fact, the $A\beta_{1-42}$ peptide induces ER dysregulation in several neuronal models (Verkhratsky and Toescu, 2003). Particularly, ER seems to play a crucial role in AD pathogenesis (Guo *et al.*,1996; Supnet *et al.*,2006; Bezprozvanny and Mattson, 2008) because it is an important site for generating Aβ fragments in neurons and because both presenilin-1 and -2 proteins are localized predominantly in this cellular compartment (Walter *et al.*,1996). Interestingly, Ca^{2+} refilling into ER seems to be a crucial early self-protective mechanism against ER stress (Verkhratsky and Toescu, 2003). In the present study, our results indicated that there exists a functional relationship between NCX3 and $[Ca^{2+}]_i$ buffering into ER. In fact, when NCX3 was silenced or knocked-out, the larger $A\beta_{1-42}$-induced ER-

Ca^{2+} accumulation was prevented, thus demonstrating the beneficial contribution of NCX3 to the ER-refilling process. In accordance with these results, in anoxic astrocytes and in Ca^{2+} oscillating muscle cells, NCX blockade prevents ER Ca^{2+} refilling (Lenart *et al.*,2004). Similarly, during OGD, the NCX1 up-regulation, in the reverse mode of operation, also plays a fundamental role in the Ca^{2+} refilling process, thus helping neurons to prevent ER stress (Fameli *et al.*,2007; Sirabella *et al.* 2009). Likewise, we found that increases in NCX3 activity seemed to delay ER stress, caspase-12 activation, apoptosis, and neuronal death triggered by $A\beta_{1-42}$. On the other hand, several lines of evidence have indicated that NCX3 plays a protective role also during OGD *in vitro* and *in vivo* thanks to its peculiar capability to maintain $[Ca^{2+}]_i$ in the physiological range (Condrescu *et al.*,1995; Linck *et al.*,1998; Pignataro *et al.*,2004; Gomez-Villafuertes *et al.*,2005; Boscia *et al.*,2006; Secondo *et al.*,2007; Molinaro *et al.*,2008).

Altogether, these data suggest that $A\beta_{1-42}$-induced up-regulation of NCX3 activity may play a fundamental role in ER Ca^{2+} refilling during $A\beta_{1-42}$ insult as it helps neurons to prevent ER stress and thus delays cell death.

This hypothesis is supported by the salient result showing that *ncx3-/-* hippocampal neurons exposed to $A\beta_{1-42}$ resulted in an earlier death. In conclusion, NCX3 activation, by calpain cleavage, might be one of the defence mechanisms against $A\beta_{1-42}$ neurotoxicity.

Although these results may appear as a paradox considering the neurotoxicity of $A\beta_{1-42}$, they may be interpreted as a survival strategy activated by neurons in an attempt to defend themselves from the death messages triggered by this peptide in the early phase of exposure.

In conclusion, even if drugs selectively activating NCX3 are in development and not yet available, this molecular target might be of clinical relevance and open a new additional strategy against AD.

6. REFERENCES

Akiyama H, Barger S, Barnum S, et al. Inflammation and Alzheimer's disease. ***Neurobiol Aging*** 2000.

Allinson, T. M., Parkin, E. T., Turner, A. J. & Hooper, N. M. ADAMs family members as amyloid precursor protein α-secretases. ***J. Neurosci. Res****.* 2003.

Amoroso S, De Maio M, Russo GM, Catalano A, Bassi A, Montagnani S, Di Renzo GF, and Annunziato L. Pharmacological evidence that the activation of the Na^{+}-Ca^{2+} exchanger protects C6 glioma cells during chemical hypoxia. ***Br J Pharmacol***, 1997.

Amoroso S, Tortiglione A, Secondo A, Catalano A, Montagnani S, Di Renzo G, and Annunziato L. Sodium nitroprusside prevents chemical hypoxia-induced cell death through iron ions stimulating the activity of the Na^{+}-Ca^{2+} exchanger in C6 glioma cells. ***J Neurochem***, 2000.

Annunziato L, Pignataro G, Di Renzo GF. Pharmacology of brain Na^{+}/Ca^{2+} exchanger: from molecular biology to therapeutic perspectives. ***Pharmacol Rev***., 2004.

Arispe N, Pollard HB, Rojas E. Giant multilevel cation channels formed by Alzheimer disease amyloid beta-protein [A beta P-(1-40)] in bilayer membranes. ***Proc Natl Acad*** **Sci U S A** 1993.

Bano D, Young KW, Guerin CJ, Lefeuvre R, Rothwell NJ, Naldini L, Rizzuto R, Carafoli E, Nicotera P Cleavage of the plasma membrane Na^{+}/Ca^{2+} exchanger in excitotoxicity. ***Cell.***, 2005.

Baumann O, Walz B: Endoplasmic reticulum of animal cells and its organization into structural and functional domains. ***Int Rev Cytol****,* 2001.

Bernales S, Papa FR, Walter P: Intracellular signaling by the unfolded protein response. ***Annu Rev Cell Dev Biol****,* 2006.

Blaustein, M.P., and Lederer, W.J. Sodium/calcium exchange: its physiological implications. ***Physiol Rev***. 1999.

Boscia F, Gala R, Pignataro G, De Bartolomeis A, Cicale M, Ambesi-Impiombato A, Di Renzo GF, Annunziato L. Permanent focal brain ischemia induces isoform-dependent changes in the pattern of Na^{+}/Ca^{2+} exchanger gene

expression in the ischemic core, periinfarct area, and intact brain regions. ***J Cereb Blood Flow Metab.***, 2006.

Breen, K. C., Bruce, M. & Anderton, B. H. β amyloid precursor protein mediates neuronal cell–cell and cell–surface adhesion. ***J. Neurosci. Res.*** 1991.

Busciglio J, Pelsman A, Wong C, et al.Altered metabolism of the amyloid beta precursor protein is associated with mitochondrial dysfunction in Down's syndrome. ***Neuron*** 2002.

Cabrejo, L. *et al.* Phenotype associated with APP duplication in five families. ***Brain*** 2006.

Caspersen C, Wang N, Yao J, et al. Mitochondrial Abeta: a potential focal point for neuronal metabolic dysfunction in Alzheimer's disease. **FASEB J** 2005.

Cheung, K.H., Shineman, D., Muller, M., Cardenas, C., Mei, L., Yang, J., Tomita, T., Iwatsubo, T., Lee, V.M., and Foskett, J.K. ***Neuron,*** 2008.

Cho C.H., S.Y. Lee, H.S. Shin, K.D. Philipson, C.O. Lee, Partial rescue of the Na+–Ca2+ exchanger (NCX1) knock-out mouse by transgenic expression of NCX1, ***Exp. Mol. Med***., 2003.

Collins TJ, Lipp P, Berridge MJ, and Bootman MD. Mitochondrial Ca^{2+} uptake depends on the spatial and temporal profile of cytosolic Ca^{2+} signals. ***J. Biol. Chem.***, 2001.

Colvin RA, Davis N, Wu A, Murphy CA, Levengood J Studies of the mechanism underlying increased Na+/Ca2+ exchange activity in Alzheimer's disease brain. ***Brain Res.,*** 1994.

Colvin, R.A., Bennett, J.W., Colvin, S.L., Allen, R.A., Martinez, J. and Milner, G.D., Na+/Ca 2+ exchange activity is increased in Alzheimer's disease brain tissues, **Brain Res***.,* 1991.

Combs CK, Karlo JC, Kao SC, Landreth GE. beta-Amyloid stimulation of microglia and monocytes results in TNFalpha-dependent expression of inducible nitric oxide synthase and neuronal apoptosis. ***J Neurosci*** 2001.

Conway S.J., A. Kruzynska-Frejtag, J. Wang, R. Rogers, P.L. Kneer, H. Chen, T. Creazzo, D.R. Menick, S.V. Koushik, Role of sodium–calcium exchanger

(Ncx1) in embryonic heart development: a transgenic rescue? ***Ann. N. Y. Acad. Sci.***, 2002.

Cook, D. G. *et al.* Alzheimer's A β(1–42) is generated in the endoplasmic reticulum/intermediate compartment of NT2N cells. ***Nature Med.*** 1997.

Cross J.L., B.P. Meloni, A. Bakker, S. Sokolow, A. Herchuelz, S. Schurmans, N.W. Knuckey, Neuronal injury in NCX3 knockout mice following permanent focal cerebral ischemia and in NCX3 knockout cortical neuronal cultures following oxygen–glucose deprivation and glutamate exposure, ***J. Exp. Stroke Transl. Med.***, 2009

Cunningham KW and Fink GR. Calcineurin inhibits VCX1-dependent H^+/C^{2+} exchange and induces Ca^{2+} ATPases in Saccharomyces cerevisiae. ***Mol Cell Bio***, 1996.

DiPolo R, Beaugé L. MgATP counteracts intracellular proton inhibition of the sodium-calcium exchanger in dialysed squid axons. ***J Physiol.,*** 2002.

DiPolo R. Calcium influx in internally dialyzed squid giant axons. ***J Gen Physiol***, 1979.

Doering AE and Lederer WJ. The action of Na+ as a cofactor in the inhibition by cytoplasmic protons of the cardiac Na^+-Ca^{2+} exchanger in the guinea-pig. ***J Physiol,*** 1994.

Doody RS, Gavrilova SI, Sano M, et al. Effect of dimebon on cognition, activities of daily living, behaviour, and global function in patients with mild-to-moderate Alzheimer's disease: a randomised, doubleblind, placebo-controlled study. ***Lancet*** 2008

Dreses-Werringloer, U., Lambert, J.C., Vingtdeux, V., Zhao, H., Vais, H., Siebert, A., Jain, A., Koppel, J., Rovelet-Lecrux, A., Hannequin, D., et al. ***Cell*** 2008.

Fiala M, Lin J, Ringman J, et al. Ineffective phagocytosis of amyloid-beta by macrophages of Alzheimer's disease patients. ***J Alzheimers Dis*** 2005.

Francis, R. *et al.* aph-1 and pen-2 are required for Notch pathway signaling, γ-secretase cleavage of βAPP, and presenilin protein accumulation. ***Dev. Cell*** 2002.

Fujioka Y, Fujioka Y, Hiroe K, and Matsuoka S. Regulation kinetics of Na^{+}/Ca^{2+} exchange current in guinea-pig ventricular myocytes. ***J Physiol***, 2000.

Giacomello M, Drago I, Pizzo P, and Pozzan T. Mitochondrial Ca^{2+} as a key regulator of cell life and death. ***Cell Death Differ***., 2007.

Good PF, Werner P, Hsu A, Olanow CW, Perl DP. Evidence of neuronal oxidative damage in Alzheimer's disease. ***Am J Pathol*** 1996.

Gorlach A, Klappa P, Kietzmann T: The endoplasmic reticulum: folding, calcium homeostasis, signaling, and redox control. ***Antioxid Redox Signal*** 2006.

Gotz J, Chen F, van Dorpe J, Nitsch RM. Formation of neurofibrillary tangles in P301l tau transgenic mice induced by Abeta 42 fibrils. ***Science*** 2001.

Gouras GK, Almeida CG, Takahashi RH. Intraneuronal Abeta accumulation and origin of plaques in Alzheimer's disease. **Neurobiol Aging** 2005.

Green KN, LaFerla FM. Linking calcium to Abeta and Alzheimer's disease. ***Neuron***. 2008. Review.

Green, K.N., Demuro, A., Akbari, Y., Hitt, B.D., Smith, I.F., Parker, I., and LaFerla, F.M. ***J. Cell Biol.*** 2008**.**

Green, K.N., Smith, I.F., and Laferla, F.M. ***Subcell. Biochem***., 2007.

Greene, L.A., and Tischler, A.S. Establishment of a noradrenergic clonal line of rat adrenal pheochromocytoma cells which respond to nerve growth factor. ***Proc Natl Acad Sci U S A*** , 1976.

Grundke-Iqbal, I. *et al.* Amyloid protein and neurofibrillary tangles coexist in the same neuron in Alzheimer disease. ***Proc. Natl Acad. Sci.*** 1989.

Grynkiewicz, G., Poenie, M., and Tsien, R.Y. A new generation of Ca2+ indicators with greatly improved fluorescence properties. ***J Biol Chem,*** 1985.

Guo, Q. *et al.* Increased vulnerability of hippocampal neurons to excitotoxic necrosis in presenilin-1 mutant knock-in mice. ***Nature Med.*** 1999.

Gyure, K. A., Durham, R., Stewart, W. F., Smialek, J. E. & Troncoso, J. C. Intraneuronal Aβ-amyloid precedes development of amyloid plaques in Down syndrome. ***Arch. Pathol. Lab. Med****.* 2001.

Haass C, Selkoe DJ. Soluble protein oligomers in neurodegeneration: lessons from the Alzheimer's amyloid beta-peptide. ***Nat Rev Mol Cell Biol*** 2007.

Haass, C. *et al.* The Swedish mutation causes earlyonset Alzheimer's disease by β-secretase cleavage within the secretory pathway. ***Nature Med.*** 1995.

Haass, C., Hung, A. Y., Schlossmacher, M. G., Teplow, D. B. & Selkoe, D. J. β-Amyloid peptide and a 3-kDa fragment are derived by distinct cellular mechanisms. ***J. Biol. Chem.*** 1993.

Hang TM and Hilgemann DW. Multiple transport modes of the cardiac Na^{+}/Ca^{2+} exchanger. ***Nature***, 2004.

Hartmann, T. *et al.* Distinct sites of intracellular production for Alzheimer's disease A β40/42 amyloid peptides. ***Nature Med.,*** 1997.

Hauptmann S, Keil U, Scherping I, Bonert A, Eckert A, Muller WE. Mitochondrial dysfunction in sporadic and genetic Alzheimer's disease. ***Exp Gerontol*** 2006.

He, L.P., Cleemann, L., Soldatov, N.M., and Morad, M. Molecular determinants of cAMP-mediated regulation of the Na+-Ca2+ exchanger expressed in human cell lines. ***J Physiol,*** 2003.

Hebert LE, Scherr PA, Bienias JL, Bennett DA, Evans DA. Alzheimer disease in the US population: prevalence estimates using the 2000 census. ***Arch Neurol*** 2003.

Hensley K, Carney JM, Mattson MP, et al. A model for beta-amyloid aggregation and neurotoxicity based on free radical generation by the peptide: relevance to Alzheimer disease. ***Proc Natl Acad Sci*** U S A 1994.

Hilgemann DW, Matsuoka S, Nagel GA, and Collins A. Steady-state and dynamic properties of cardiac sodium-calcium exchange. Sodium-dependent inactivation. ***J Gen Physiol***, 1992.

Hilgemann DW. Regulation and deregulation of cardiac Na^{+}/Ca^{2+} exchange in giant excised sarcolemmal membrane patches. ***Nature***, 1990.

Hirai K, Aliev G, Nunomura A, et al.Mitochondrial abnormalities in Alzheimer'sdisease. ***J Neurosci*** 2001.

Hoozemans JJ, Veerhuis R, Van Haastert ES, et al. The unfolded protein response is activated in Alzheimer's disease. ***Acta Neuropathol*** 2005

Hoozemans JJM, van Haastert ES, Nijholt DAT, Rozemuller AJM, Eikelenboom P, Scheper W: The unfolded protein response is activated in pretangle neurons in Alzheimer's disease hippocampus. *Am J Pathol,* 2009.

Humphries KM, Szweda LI. Selective inactivation of alpha-ketoglutarate dehydrogenase and pyruvate dehydrogenase: reaction of lipoic acid with 4-hydroxy-2-nonenal. ***Biochemistry***, 1998.

Hussain, I. *et al.* Identification of a novel aspartic protease (Asp 2) as β-secretase. ***Mol. Cell. Neurosci.,*** 1999.

Isaacs AM, Senn DB, Yuan M, Shine JP, Yankner BA. Acceleration of amyloid beta-peptide aggregation by physiological concentrations of calcium. ***J Biol Chem*** 2006.

Iwamoto T, Pan Y, Nakamura TY, Wakabayashi S, and Shigekawa M. Protein kinase C-dependent regulation of Na^+/Ca^{2+} exchanger isoforms NCX1 and NCX3 does not require their direct phosphorylation. ***Biochemistry***, 1998.

Iwamoto T, Pan Y, Wakabayashi S, Imagawa T, Yamanaka HI, and Shigekawa M. Phosphorylation-dependent regulation of cardiac Na^+/Ca^{2+} exchanger via protein kinase C ***J Biol Chem***, 1996.

Iwamoto T, Wakabayashi S, and Shigekawa M. Growth factor-induced phosphorylation and activation of aortic smooth muscle Na^+/Ca^{2+} exchanger. ***J Biol Chem***, 1995.

Jankowsky, J. L. *et al.* Mutant presenilins specifically elevate the levels of the 42 residue β-amyloid peptide *in vivo*: evidence for augmentation of a 42-specific γ secretase. ***Hum. Mol. Genet.***2004.

Jarrett, J. T., Berger, E. P. & Lansbury, P. T. Jr. The carboxy terminus of the β amyloid protein is critical for the seeding of amyloid formation: implications for the pathogenesis of Alzheimer's disease. ***Biochemistry*** 1993.

Jeon D., Y.-M. Yang, M.-J. Jeong, K.D. Philipson, H. Rhim, H.-S. Shin, Enhanced learning and memory in mice lacking Na+/Ca2+ exchanger 2, ***Neuron***, 2003.

Kayed R, Head E, Thompson JL, et al. Common structure of soluble amyloid oligomers implies common mechanism of pathogenesis. ***Science*** 2003.

Keller JN, Mark RJ, Bruce AJ, et al. 4-Hydroxynonenal, an aldehydic product of membrane lipid peroxidation, impairs glutamate transport and mitochondrial function in synaptosomes. ***Neuroscience*** 1997.

Kiedrowski L. N-methyl-D-aspartate excitotoxicity: relationships among plasma membrane potential, Na^+/Ca^{2+} exchange, mitochondrial Ca^{2+} overload, and cytoplasmic concentrations of Ca^{2+}, H^+, and K^+. ***Mol Pharmacol***, 1999.

Kim I, Xu W, Reed JC: Cell death and endoplasmic reticulum stress: disease relevance and therapeutic opportunities. ***Nat Rev Drug Discov****,* 2008.

Kinoshita, A. *et al.* Demonstration by FRET of BACE interaction with the amyloid precursor protein at the cell surface and in early endosomes. ***J. Cell Sci.*** 2003.

Klein WL, Krafft GA, Finch CE. Targeting small Abeta oligomers: the solution to an Alzheimer's disease conundrum? ***Trends Neurosci*** 2001.

Ko MH, Puglielli L: Two endoplasmic reticulum (ER)/ER Golgi intermediate compartment-based lysine acetyltransferases post-translationally regulate BACE1 levels. ***J Biol Chem****,* 2009.

Kojro, E. & Fahrenholz, F. The non-amyloidogenic pathway: structure and function of α-secretases. ***Subcell. Biochem.*** **38**, 105–127 (2005).

Koushik S.V., J. Wang, R. Rogers, D. Moskophidis, N.A. Lambert, T.L. Creazzo, S.J. Conway, Targeted inactivation of the sodium–calcium exchanger (Ncx1) results in the lack of a heartbeat and abnormal myofibrillar organization, ***FASEB J***., 2001.

LaFerla FM, Green KN, **Oddo** S. Intracellular amyloid-beta in Alzheimer's disease. ***Nat Rev Neurosci.*** 2007 Jul. **Review**.

LaFerla FM. Calcium dyshomeostasis and intracellular signalling in Alzheimer's disease. ***Nat Rev Neurosci*** 2002.

Lankiewicz, S., Luetjens, M.C., Truc Bui, N., Krohn, A.J., Poppe, M., Cole, G.M., Saido, T.C., and Prehn, J.H. Activation of calpain I converts excitotoxic neuron death into a caspase-independent cell death. ***J. Biol. Chem***., 2000.

Lee, S. J. *et al.* A detergent-insoluble membrane compartment contains Aβ *in vivo*. ***Nature Med.,*** 1998.

Leissring MA, Akbari Y, Fanger CM, Cahalan MD, Mattson MP, LaFerla FM. Capacitative calcium entry deficits and elevated luminal calcium content in mutant presenilin-1 knockin mice. ***J Cell Biol*** 2000.

Leissring, M.A., Paul, B.A., Parker, I., Cotman, C.W., and LaFerla, F.M. ***J. Neurochem.***, 1999.

Leist, M., Volbracht, C., Kuhnle, S., Fava, E., Ferrando-May, E., and Nicotera, P. Caspase-mediated apoptosis in neuronal excito-toxicity triggered by nitric oxide. ***Mol. Med***., 1997.

Levitan, D. *et al.* PS1 N- and C-terminal fragments form a complex that functions in APP processing and Notch signaling. ***Proc. Natl Acad. Sci****.* 2001.

Lewis J, Dickson DW, Lin WL, et al. Enhanced neurofibrillary degeneration in transgenic mice expressing mutant tau and APP. **Science** 2001

Li Y, Liu L, Barger SW, Griffin WS. Interleukin-1 mediates pathological effects of microglia on tau phosphorylation and on synaptophysin synthesis in cortical neurons through a p38-MAPK pathway. ***J Neurosci*** 2003.

Li Z, Matsuoka S, Hryshko LV, Nicoll DA, Bersohn MM, and Burke EP. Cloning of the NCX2 isoform of the plasma membrane Na^{+}-Ca^{2+} exchanger. ***J Biol Chem***, 1994.

Lin H, Bhatia R, Lal R. Amyloid beta protein forms ion channels: implications for Alzheimer's disease pathophysiology. ***FASEB J*** 2001

Linck B, Qiu Z, He Z, Tong Q, Hilgemann DW, and Philipson KD. Functional comparison of the three isoforms of the Na+/Ca^{2+} exchanger (NCX1, NCX2, NCX3). ***Am J Physiol,*** 1998.

López Salon M, Morelli L, Casta.o EM, Soto EF, Pasquini JM. Defective ubiquitination of cerebral proteins in Alzheimer's disease. ***J Neurosci Res*** 2000.

Lue LF, Kuo YM, Roher AE, et al. Soluble amyloid beta peptide concentration as a predictor of synaptic change in Alzheimer's disease. ***Am J Pathol***, 1999.

Lytton J, Li XF, Dong H, and Kraev A. K^{+}-dependent Na^{+}/Ca^{2+} exchangers in the brain. ***Ann N Y Acad Sci,*** 2002.

Mark RJ, Pang Z, Geddes JW, Uchida K, Mattson MP. Amyloid beta-peptide impairs glucose transport in hippocampal and cortical neurons: involvement of membrane lipid peroxidation. **J Neurosci** 1997.

Martinon F, Mayor A, Tschopp J: The inflammasomes: guardians of the body. ***Annu Rev Immunol*** 2009.

Mason, R.P., Shoemaker, W.J., Shajenko, L., Chambers, T.E. and Herbette, L.G., Evidence for changes in the Alzheimer's disease brain cortical membrane structure mediated by cholesterol, ***Neurobiol. Aging****,* 1992.

Matsuoka S, Nicoll DA, He Z, and Philipson KD. Regulation of cardiac Na^{+}-Ca^{2+} exchanger by the endogenous XIP region. ***J Gen Physiol***, 1997.

McGeer EG, Yasojima K, Schwab C, McGeer PL. The pentraxins: possible role in Alzheimer's disease and other innate inflammatory diseases. ***Neurobiol Aging*** 2001.

McGeer PL, McGeer EG. NSAIDs and Alzheimer disease: epidemiological, animal model and clinical studies. ***Neurobiol Aging*** 2007.

McLaurin J, Kierstead ME, Brown ME, et al. Cyclohexanehexol inhibitors of Abeta aggregation prevent and reverse Alzheimer phenotype in a mouse model. ***Nat Med*** 2006

Mellgren, R.L., Renno, W.M., and Lane, R.D. The non-lyso- cultured cerebellar granule cells. ***J. Neurosci.***, 1989.

Mizuguchi, M., Ikeda, K. & Kim, S. U. Differential distribution of cellular forms of β-amyloid precursor protein in murine glial cell cultures. ***Brain Res.*** 1992.

Molinaro P., O. Cuomo, G. Pignataro, F. Boscia, R. Sirabella, A. Pannaccione, A. Secondo, A. Scorziello, A. Adornetto, R. Gala, D. Viggiano, S. Sokolow, A. Herchuelz, S. Schurmans, G. Di Renzo, L. Annunziato, Targeted disruption of Na+/Ca2+ exchanger 3 (NCX3) gene leads to a worsening of ischemic brain damage, ***J. Neurosci***., 2008.

Mori, C. *et al.* Intraneuronal Aβ42 accumulation in Down syndrome brain. ***Amyloid*** 2002.

Mungarro-Menchaca X, Ferrera P, Moran J, Arias C. beta-Amyloid peptide induces ultrastructural changes in synaptosomes and potentiates mitochondrial dysfunction in the presence of ryanodine. ***J Neurosci Res*** 2002.

Murachi, T., Hatanaka, M., and Hamakubo, T. Calpains and neuroeptide metabolism. In Neuropeptides and Their Peptidases, ***A.J. Turner, ed.,*** 1987.

Nadiri A, Wolinski MK, Saleh M: The inflammatory caspases: key players in the host response to pathogenic invasion and sepsis. ***J Immunol****,* 2006.

Nelson O, Tu H, Lei T, Bentahir M, de Strooper B, Bezprozvanny I. Familial Alzheimer disease-linked mutations specifically disrupt Ca2+ leak function of presenilin 1. ***J Clin Invest*** 2007.

Neumar, R.W., Xu, Y.A., Gada, H., Guttmann, R.P., and Siman, R. Cross-talk between calpain and caspase proteolytic systems during neuronal apoptosis. ***J. Biol. Chem***., *2003.*

Nicoll DA, Hryshko LV, Matsuoka S, Frank JS, and Philipson KD. Mutation of amino acid residues in the putative transmembrane segments of the cardiac sarcolemmal Na^+-Ca^{2+} exchanger. ***J Biol Chem***, 1996.

Nicoll DA, Longoni S, and Philipson KD. Molecular cloning and functional expression of the cardiac sarcolemmal Na^+-Ca^{2+}exchanger. ***Science***, 1990.

Nicoll DA, Ottolia M, Lu L, Lu Y, and Philipson KD. A new topological model of the cardiac sarcolemmal Na^+-Ca^{2+} exchanger. ***J Biol Chem***, 1999.

Nilsberth, C. *et al.* The 'Arctic' APP mutation (E693G) causes Alzheimer's disease by enhanced Aβ protofibril formation. ***Nature Neurosci.*** 2001.

Nunomura A, Perry G, Aliev G, et al. Oxidative damage is the earliest event in Alzheimer disease. ***J Neuropathol Exp Neurol*** 2001.

Oddo S, Caccamo A, Shepherd JD, et al. Triple-transgenic model of Alzheimer's disease with plaques and tangles: intracellular Abeta and synaptic dysfunction. ***Neuron*** 2003

Peterson, C., Changes in calcium's role as a messenger during aging in neuronal and non-neuronal cells, ***Ann. NYAcad. Sci.,*** 1992.

Philipson KD and Nicoll DA. Sodium-calcium exchange: a molecular perspective. ***Ann Rev Physiol***, 2000.

Philipson KD, Longoni S and Ward R. Purification of the cardiac Na^+-Ca^{2+} exchange protein. ***Biochim Biophys Acta***, 1988.

Pierrot N, Ghisdal P, Caumont AS, Octave JN. Intraneuronal amyloid-beta1-42 production triggered by sustained increase of cytosolic calcium concentration induces neuronal death. ***J Neurochem*** 2004.

Pignataro G, Gala R, Cuomo O, Tortiglione A, Giaccio L, Castaldo P, Sirabella R, Matrone C, Canitano A, Amoroso S, Di Renzo G and Annunziato L. Two

sodium/calcium exchanger gene products, NCX1 and NCX3, play a major role in the development of permanent focal cerebral ischemia. ***Stroke***, 2004.

Quednau BD, Nicoll DA, and Philipson KD. Tissue specificity and alternative splicing of the Na^{+}/Ca^{2+} exchanger isoforms NCX1, NCX2 and NCX3 in rat. ***Am J Physiol***, 1997.

Querfurth HW, **LaFerla** FM, Alzheimer's disease.***N Engl J Med***. 2010 Jan 28; Review. Erratum in: ***N Engl J Med.*** 2011 Feb 10

Ranciat-McComb N.S., K.S. Bland, J. Huschenbett, L. Ramonda, M. Bechtel, A. Zaidi, M.L. Michaelis, Antisense oligonucleotide suppression of Na+/Ca2+ exchanger activity in primary neurons from rat brain, ***Neurosci. Lett.***, 2000.

Reddy PH, Beal MF. Amyloid beta, mitochondrial dysfunction and synaptic damage: implications for cognitive decline in aging and Alzheimer's disease. ***Trends Mol Med*** 2008.

Reeves JP and Hale CC The stoichiometry of the cardiac sodium-calcium exchange system. ***J Biol Chem***,1984.

Reeves JP, Bailey CA and Hale CC. Redox modification of sodium-calcium exchange activity in cardiac sarcolemmal vesicles. ***J Biol Chem***, 1986.

Robles, E., Huttenlocher, A., and Gomez, T.M. (2003). Filopodial calcium transients regulate growth cone motility and guidance through local activation of calpain. ***Neuron***, 2003.

Ron D, Walter P: Signal integration in the endoplasmic reticulum unfolded protein response. ***Nat Rev Mol Cell Biol*** 2007.

Rothman SM, Olney JW. Excitotoxicity and the NMDA re4ptor — still lethal after eight years. ***Trends Neurosci*** 1995.

Rovelet-Lecrux, A. *et al.* APP locus duplication causes autosomal dominant early-onset Alzheimer disease with cerebral amyloid angiopathy. ***Nature Genet.*** 2006.

Rybalchenko, V., Hwang, S.Y., Rybalchenko, N., and Koulen, P. ***Int. J. Biochem. Cell Biol.***, 2008.

Sabo, S. L., Ikin, A. F., Buxbaum, J. D. & Greengard, P. The Alzheimer amyloid precursor protein (APP) and FE65, an APP-binding protein, regulate cell movement. ***J. Cell Biol.*** 2001.

Schnetkamp PP, Basu DK, and Szerencsei RT. Na^{+}/Ca^{2+} exchange in bovine rod outer segments requires and transports K^{+}. ***Am J Physiol***, 1989.

Schroder M, Kaufman RJ: The mammalian unfolded protein response. ***Annu Rev Biochem,*** 2005.

Schulze DH, Muqhal M, Lederer WJ, and Ruknudin AM. Sodium/calcium exchanger (NCX1) macromolecular complex. ***J Biol Chem,*** 2003.

Schwab BL, Guerini D, Didszun C, Bano D, Ferrando-May E, Fava E, Tam J, Xu D, Xanthoudakis S, Nicholson DW, Carafoli E, Nicotera P. Cleavage of plasma membrane calcium pumps by caspases: a link between apoptosis and necrosis. ***Cell Death Differ***, 2002.

Scorziello, A., Pellegrini, C., Forte, L., Tortiglione, A., Gioielli, A., Iossa, S., Amoroso, S., Tufano, R., Di Renzo, G., and Annunziato, L. Differential vulnerability of cortical and cerebellar neurons in primary culture to oxygen glucose deprivation followed by reoxygenation. ***J Neurosci Res,*** 2001.

Secondo A, Molinaro P, Pannaccione A, Esposito A, Cantile M, Lippiello P, Sirabella R, Iwamoto T, Di Renzo G, Annunziato L. Nitric Oxide stimulates NCX1 and NCX2 but inhibits NCX3 isoform by three distinct molecular determinants. ***Mol Pharmacol***. 2010.

Secondo A, Staiano RI, Scorziello A, Sirabella R, Boscia F, Adornetto A, Valsecchi V, Molinaro P, Canzoniero LM, Di Renzo G, Annunziato L. BHK cells transfected with NCX3 are more resistant to hypoxia followed by reoxygenation than those transfected with NCX1 and NCX2: Possible relationship with mitochondrial membrane potential. ***Cell Calcium***, 2007.

Selkoe DJ. Alzheimer's disease: genes, proteins, and therapy. ***Physiol Rev*** 2001.

Shaul O, Hilgemann DW, de-Almeida-Engler J, Van Montagu M, Inz D, and Galili G. Cloning and characterization of a novel $Mg^{(2+)}/H^{(+)}$ exchanger. ***EMBO*** (Eur Mol Biol Organ) J, 1999.

Siemers ER, Quinn JF, Kaye J, et al. Effects of a gamma-secretase inhibitor in a randomized study of patients with Alzheimer disease. ***Neurology***, 2006

Siman, R., and Noszek, J.C. Excitatory amino acids activate calpain I and induce structural protein breakdown in vivo. ***Neuron,*** 1988.

Simard AR, Soulet D, Gowing G, Julien JP, Rivest S. Bone marrow-derived microglia play a critical role in restricting senile plaque formation in Alzheimer's disease. ***Neuron*** 2006.

Sinha, S. *et al.* Purification and cloning of amyloid precursor protein β-secretase from human brain. ***Nature*** 1999.

Sirabella R, Secondo A, Pannaccione A, Scorziello A, Valsecchi V, Adornetto A, Bilo L, Di Renzo G, Annunziato L. Anoxia-induced NF-kappaB-dependent upregulation of NCX1 contributes to Ca^{2+} refilling into endoplasmic reticulum in cortical neurons. ***Stroke***, 2009.

Skovronsky, D. M., Doms, R. W. & Lee, V. M. Detection of a novel intraneuronal pool of insoluble amyloid β protein that accumulates with time in culture. ***J. Cell Biol.,*** 1998.

Smith MA, Perry G, Richey PL, et al. Oxidative damage in Alzheimer's. ***Nature*** 1996.

Smith MA, Richey Harris PL, Sayre LM, Beckman JS, Perry G. Widespread peroxynitrite peroxynitrite-mediated damage in Alzheimer's disease. ***J Neurosci*** 1997.

Smith, I.F., Hitt, B., Green, K.N., Oddo, S., and LaFerla, F.M. ***J. Neurochem.,*** 2005.

Sokolow S.,M.Manto, P. Gailly, J. Molgo, C. Vandebrouck, J.M. Vanderwinden, A.Herchuelz, S. Schurmans, Impaired neuromuscular transmission and skeletal muscle fiber necrosis in mice lacking Na/Ca exchanger 3, ***J. Clin. Invest***., 2004.

St George-Hyslop, P. H. & Petit, A. Molecular biology and genetics of Alzheimer's disease. ***C. R. Biol.,*** 2005.

Steiner, H. *et al.* PEN-2 is an integral component of the γ-secretase complex required for coordinated expression of presenilin and nicastrin. ***J. Biol. Chem.,*** 2002

Tanzi RE, Bertram L. Twenty years of the Alzheimer's disease amyloid hypothesis: a genetic perspective. ***Cell*** 2005.

Thinakaran G, Koo EH: Amyloid precursor protein trafficking, processing, and function. ***J Biol Chem,*** 2008.

Tu, H., Nelson, O., Bezprozvanny, A., Wang, Z., Lee, S.F., Hao, Y.H., Serneels, L., De Strooper, B., Yu, G., and Bezprozvanny, I. ***Cell***, 2006.

Vassar, R. *et al.* β-secretase cleavage of Alzheimer's amyloid precursor protein by the transmembrane aspartic protease BACE. ***Science*****,** 1999.

Vlad SC, Miller DR, Kowall NW, Felson DT. Protective effects of NSAIDs on the development of Alzheimer disease. ***Neurology*** 2008.

Wakimoto K., H. Fujimura, T. Iwamoto, T. Oka, K. Kobayashi, S. Kita, S. Kudoh, M. Kuro-o, Nabeshima Y-i, M. Shigekawa, Y. Imai, I. Komuro, Na+/Ca2+ exchangerdeficient mice have disorganized myofibrils and swollen mitochondria in cardiomyocytes, ***Comp. Biochem. Physiol. B: Biochem. Mol. Biol***., 2003.

Walsh DM, Selkoe DJ. A beta oligomers — a decade of discovery. ***J Neurochem*** 2007.

Wild-Bode, C. *et al.* Intracellular generation and accumulation of amyloid beta-peptide terminating at amino acid 42. ***J. Biol. Chem.,*** 1997.

Wolfe, M. S. *et al.* Two transmembrane aspartates in presenilin-1 required for presenilin endoproteolysis and γ-secretase activity. ***Nature****,* 1999.

Wu A, Derrico CA, Hatem L, and Colvin RA Alzheimer's amyloid-beta peptide inhibits sodium/calcium exchange measured in rat and human brain plasma membrane vesicles. ***Neuroscience***, 1997.

Wyss-Coray T, Mucke L. Inflammation in neurodegenerative disease — a double-edged sword. ***Neuron*** 2002.

Xu, H., Greengard, P. & Gandy, S. Regulated formation of Golgi secretory vesicles containing Alzheimer β-amyloid precursor protein. ***J. Biol. Chem.*** 1995.

Yan SD, Chen X, Fu J, et al. RAGE and amyloid-beta peptide neurotoxicity in Alzheimer's disease. ***Nature*** 1996.

Younkin, S. G. The role of Aβ 42 in Alzheimer's disease. ***J. Physiol. Paris*****,** 1998.

Yu, G. *et al.* Nicastrin modulates presenilin-mediated notch/glp-1 signal transduction and βAPP processing.***Nature*** 2000.

Zatti, G., Burgo, A., Giacomello, M., Barbiero, L., Ghidoni, R., Sinigaglia, G., Florean, C., Bagnoli, S., Binetti, G., Sorbi, S., et al. ***Cell Calcium,*** 2006.